

**PREDICTION OF THE MOST EFFECTIVE PLACEMENT  
OF GROYNES AT A RIVER BEND USING ANSYS FLUENT**

A Dissertation submitted in partial fulfillment of the requirement for the  
Award of degree of

**MASTER OF TECHNOLOGY  
IN  
HYDRAULICS & FLOOD ENGINEERING**

**BY**

**SIDDHARTHA CHOWDHARY  
(ROLL NO. 2K13/HFE/05)**

**Under the Guidance of**

**Dr. RAKESH KUMAR**

**Professor**

**Department of Civil Engineering  
Delhi Technological University  
Delhi**



**DELHI TECHNOLOGICAL UNIVERSITY  
(FORMERLY DELHI COLLEGE OF ENGINEERING)**

**DELHI - 110042**

**July-2015**



## **CANDIDATE'S DECLARATION**

I do hereby certify that the work presented is the report entitled “**Prediction of the most effective placement of groynes at a river bend using Ansys Fluent**” in the partial fulfillment of the requirements for the award of the degree of “Master of Technology” in Hydraulics & Flood engineering submitted in the Department of Civil Engineering, Delhi Technological University, is an authentic record of our own work carried out from January 2015 to July 2015 under the supervision of Dr. Rakesh Kumar (Professor), Department of Civil Engineering.

I have not submitted the matter embodied in the report for the award of any other degree or diploma.

Siddhartha Chowdhary

Date: 31/7/15

(2K13/HFE/05)

---

## **CERTIFICATE**

This is to certify that above statement made by the candidate is correct to best of my knowledge.

Dr. Rakesh Kumar  
(Professor)  
Department of Civil Engineering  
Delhi Technological University

## **ACKNOWLEDGEMENT**

I take this opportunity to express my profound gratitude and deep regards to Dr. Rakesh Kumar (Professor, Civil Engineering Department, DTU ) for his exemplary guidance, monitoring and constant encouragement throughout the course of this project work. The blessing, help and guidance given by him from time to time shall carry me a long way in life on which I am going to embark.

I would also like to thank Dr. Nirendra Dev (Head of Department, Civil Engineering Department, DTU) for extending his support and guidance.

Professors and faculties of the Department of Civil Engineering, DTU, have always extended their full co-operation and help. They have been kind enough to give their opinions on the project matter; I am deeply obliged to them. They have been a source of encouragement and have continuously been supporting me with their knowledge base, during the study. Several of well-wishers extended their help to me directly or indirectly and we are grateful to all of them without whom it would have been impossible for me to carry on my work.

## **ABSTRACT**

In a meandering river the most critical section of the river is when it changes its curvature, at this section complex flow takes place, also the additional forces like the centrifugal force that come into play due to the curvature make the bank protection against scouring essential. The influence factors of spur are largely related to the stream characteristics, hydrologic variables, hydraulic characteristics and local variables. So the analysis considering all the involved factors becomes very extensive. There are very few studies that concentrate on the analysis of flow in a channel bend, owing to the complexities. Simulating the curvature and river conditions in a flume is also tough, fortunately making use of computational dynamic software help in simulation studies. In this study groynes at different position on the channel bend are analyzed using ANSYS Fluent software. The turbulence model used was standard k-epsilon model for the flow. Four different lengths of spurs were taken i.e. 2.5m, 3m, 3.5m, 4m. The groynes were placed at six different positions. Furthermore three different approach velocities were taken i.e. 2.6m/s, 2m/s and 1.4m/s. So in total 72 different combinations of cases were undertaken and the results analyzed. The tip velocities, protected length and bed shear stress were compared for different positions of groyne. Multiple linear regression has been used to see the relationship and correlation between the maximum bed shear stress, tip velocity, protected length, groyne length and position of groyne. The most effective position of the groyne among the six cases was suggested in this study, also suggestions were made for the appropriate length of groyne.

# CONTENTS

<b>Title</b>	<b>Page No.</b>
<b>CANDIDATE'S DECLARATION</b>	<b>ii</b>
<b>ACKNOWLEDGEMENT</b>	<b>iii</b>
<b>ABSTRACT</b>	<b>iv</b>
<b>LIST OF FIGURES</b>	<b>viii</b>
<b>LIST OF TABLES</b>	<b>x</b>
<b>LIST OF SYMBOLS</b>	<b>xi</b>
1. INTRODUCTION	1
1.1 FOREWORD	1
1.2 AIM OF STUDY	1
1.3 INSPIRATION	1
1.4 BACKGROUND	2
1.4.1 FLOW IN A CHANNEL	2
1.5 RESEARCH STRATEGY	3
1.5.1 CHANNEL AND GROUYNE DESCRIPTION	3
1.6 RESEARCH CONSTRAINT	4
1.7 ORGANIZATION OF DISSERTATION	4
2. LITERATURE REVIEW	5
2.1 INTRODUCTION	5
2.2 GROYNES IN A BEND – EXPERIMENTAL STUDIES	5
2.2.1 VELOCITY DISTRIBUTION PATTERNS	5
2.2.2 RECIRCULATION PATTERNS	6
2.3 GROYNES IN A BEND –NUMERICAL STUDIES	7
2.3.1 HELICAL FLOW PATTERNS	7
2.3.2 SHEAR STRESS DISTRIBUTIONS	8

2.3.3 VORTICITY DISTRIBUTIONS	9
2.4 NECESSITY OF LITERATURE REVIEW	9
3. METHODOLOGY	10
3.1 SYNOPSIS OF SIMULATION	10
3.2 CHANNEL CHARACTERISRICS	10
3.3 GROYNE CHARACTERISTICS	10
3.4 POINTS OF OBSERVATION	11
3.5 INPUT VARIABLES	12
3.6 MEASUREMENTS	12
3.6.1 PROTECTED LENGTH	12
3.6.2 VELOCITY	13
3.6.3 SHEAR STRESS	
3.7 SOFTWARE INPUT	13
3.7.1 GEOMETRY	13
3.7.2 MESHING	15
3.7.3 SETUP	16
3.7.4 SOLUTION	17
4. NUMERICAL DATA	18
4.1 INTRODUCTION	18
4.2 EXPERIMENTAL DATA/SOFTWARE OUTPUT	19
4.3 PLOTS OBTAINED FROM ANSYS FLUENT (CFD –POST)	27
4.3.1 STREAMLINES	27
4.3.2 VELOCITY VECTORS	28
4.3.3 CONTOURS OF VELOCITY IN MODEL SPACE	30
4.3.4 CONTOURS OF BED SHEAR STRESS	31
5. RESULTS AND ANALYSIS	33
5.1 INTRODUCTION	33

5.2 FACTORS AFFECTING THE FLOW IN A RIVER BEND	33
5.3 REGRESSION ANALYSIS	33
5.3.1 REGRESSION FOR PROTECTED LENGTH	34
5.3.2 REGRESSION FOR TIP VELOCITY	36
5.3.3 REGRESSION FOR MAXIMUM SHEAR STRESS	39
5.3.4 CONCLUSION	37
5.4 VARIATION OF FACTOR $V_{tip}/V_{app}$ WITH FACTOR L/B	41
5.5 VARIATION OF FACTOR $\tau_{max}$ FOR GROUYNE POSITIONS	43
5.6 SUMMARY	44
6. CONCLUSION	45
6.1 INTRODUCTION	45
6.2 CONCLUSIONS BASED ON PROTECTED LENGTH	45
6.3 CONCLUSIONS BASED ON TIP VELOCITY	45
6.4 CONCLUSIONS BASED ON MAXIMUM BED SHEAR STRESS	46
6.5 SUGGESTION FOR THE BEST PLACEMENT OF GROYNES	46
6.6 FURTHER IMPROVEMENTS	46
<b>REFERENCES/BIBLIOGRAPHY</b>	<b>44</b>

## LIST OF FIGURES

Figure No.	Title	Page No.
FIG 1.1	Helical flow in bend	2
FIG 1.2	Radial Force Balance	3
FIG 2.1	Recirculation region downstream of a groyne between the separation and reattachment point.	6
FIG 2.2	Recirculation region downstream of the groyne on concave face of bend in this study using Ansys.	6
FIG 2.3	a) Channel cross-section showing secondary helical flow pattern in 90° bend without groyne and b) with groynes.	8
FIG 2.4	Maximum bed shear stress near the groyne tips.	8
FIG 3.1	Orientation of groyne placement with respect to a fixed meridian “OP”.	11
FIG 3.2	Protected length corresponding to safe bank length.	12
FIG 3.3	Dialog box showing basic components of Ansys Fluent.	13
FIG 3.4	Channel Geometry as looks in Design Modular of Ansys Fluent	14
FIG 3.5	Channel Geometry as it looks in AutoCAD 2013/	14
FIG 3.6	Meshing by Cut Cell Assembly method with relevance to proximity and curvature.	15
FIG 3.7	Definition of mathematical model used, k-epsilon.	16
FIG 3.8	One of the case of this study where the solution converged at 200 <sup>th</sup> iteration.	17
FIG 4.1	Streamlines for groyne position “A” that is attracting at 0° and repelling at 10°, wrt decided meridian “OP”.	27
FIG 4.2	Streamlines for groyne position “D” that is attracting at 5° and repelling at 30°, wrt decided meridian “OP”.	27
FIG 4.3	Streamlines for groyne position “E” that is attracting at 20° and repelling at 45°, wrt decided meridian “OP”.	28
FIG 4.4	Velocity vectors for groyne position “A” that is attracting at 0° and repelling at 10° wrt decided meridian “OP”	28



FIG 4.5	Velocity vectors for groyne position “D” that is attracting at $5^0$ & repelling at $30^0$ , wrt decided meridian “OP”.	29
FIG 4.6	Velocity vectors for groyne position “E” that is attracting at $20^0$ & repelling at $45^0$ , wrt decided meridian “OP”.	29
FIG 4.7	Velocity contours for groyne position “A” that is attracting at $0^0$ & repelling at $10^0$ , wrt decided meridian “OP”.	30
FIG 4.8	Velocity contours for groyne position “D” that is attracting at $5^0$ & repelling at $30^0$ , wrt decided meridian “OP”.	30
FIG 4.9	Velocity contours for groyne position “E” that is attracting at $20^0$ & repelling at $45^0$ , wrt decided meridian “OP”.	31
FIG 4.10	Bed shear stress contours for groyne position “A” that is attracting at $0^0$ and repelling at $10^0$ , wrt to decided meridian “OP”	31
FIG 4.11	Bed shear stress contours for groyne position “D” that is attracting at $5^0$ and repelling at $30^0$ , wrt decided meridian “OP”.	32
FIG 4.12	Bed shear stress contours for groyne position “E” that is attracting at $20^0$ and repelling at $45^0$ , wrt decided meridian “OP”.	32
FIG 5.1	Variation of $V_{tip}/V_{app}$ with L/B for velocity 1.4m/s.	41
FIG 5.2	Variation of $V_{tip}/V_{app}$ with L/B for velocity 2 m/s.	41
FIG 5.3	Variation of $V_{tip}/V_{app}$ with L/B for velocity 2.6 m/s.	42
FIG 5.4	$\tau_{max}$ for groyne size 3.5m a) velocity 2.6m/s b) velocity 2m/s.	43
FIG 5.5	$\tau_{max}$ for groyne size 3m a) velocity 2.6m/s b) velocity 2m/s.	43
FIG 5.6	$\tau_{max}$ for groyne size 2.5m a) velocity 2.6m/s b) velocity 2m/s.	44

## LIST OF TABLES

<b>Table No.</b>	<b>Title</b>	<b>Page No.</b>
TABLE 1.1	Field studies of groynes in channel bends.	3
TABLE 3.1	Position of different groyne.	11
TABLE 3.2	Meshing Components and the assigned values/method for study.	15
TABLE 3.3	Boundary Condition for each case of observation.	16
TABLE 3.4	Solution Methods Used in this study.	17
TABLE 4.1	Positions of groyne combination and the symbol used.	18
TABLE 4.2	Values of tip velocity ( $V_{tip}$ ) and maximum velocity ( $V_{max}$ ), Froude number and derived parameters	19
TABLE 4.3	Values of protected length (D) and groyne length (L).	21
TABLE 4.4	Values of maximum shear stress and initial shear stress (undisturbed) and derived factors	24

## **LIST OF SYMBOLS**

<b>Symbol</b>	<b>Title</b>
$S_r$	Surface Slope
$g$	Gravitational acceleration
$V_{app}$	Velocity of approach.
$V_{tip}$	Tip velocity
$\tau_{max}$	Maximum bed shear stress
$\tau_o$	Initial (undisturbed) bed shear stress
Fr.	Froude Number
D	Protected length
L	Length of groyne
$V_{max}$	Absolute maximum velocity
R	Mean radius of curvature

# CHAPTER 1

## INTRODUCTION

### 1.1 FOREWORD

Groynes are flow diversion structures, commonly used in river engineering to prevent bank erosion and control river meandering. They may serve additional functions such as improving channel navigability by deepening the river centreline; for training the river in a designated path; aiding in flood management and to maintain equilibrium of suspended and settled alluvium.

Groynes perform three main functions, they deflect flow and secondary currents away from the river bank, they disrupt high velocity gradients in the near bank region, and they shift the thalweg closer to the channel centreline (Matsuura and Townsend 2004). In this way they may provide a longer-term solution to mitigate bank migration (Mosselman *et al.* 2000)

For the purpose of bank protection, it is best for them to be pointed in the upstream direction. Commonly they are also referred to in the literature as spur dykes, rock vanes, weirs and stream barbs. Normally constructed from rock, they may be submerged or emergent with respect to normal water levels.

### 1.2 AIM OF STUDY

The objective of this study is to analyse the velocity flow patterns, protection length, shear stresses due to introduction of groyne in a channel bend and as a result decide factors that influence the effective placement by suitable combination of groynes.

### 1.3 INSPIRATION

The protection of banks of a meandering river, where curvature is high, is conventionally done by providing structures like groyne on just the concave face of the bank. They are usually provided in series over the length of the bank.

Ansys Fluent, is a remarkable tool that allowed to design a channel and simulate a flow in it, and apply numerous iterations. This allows to study cases of different flows through the bend and the results made to move in this direction.

By employing groynes not just on the concave face but also on the convex face it was noticed that this could also be a possible area of research. After searching for the relevant literature this dissertation was taken up.

## 1.4 BACKGROUND

### 1.4.1 FLOW IN A CHANNEL BEND

Flow in a channel bend is more complex than in a straight channel. This is partly due to the presence of helical flow patterns induced by centrifugal forces. As flow enters the bend, it is acted upon by centrifugal forces which push it towards the outer bank (Figure 1.1). Since the magnitudes of surface velocities are greater than those at the bed, surface velocities experience a greater centrifugal force, and therefore move faster towards the outer bank than bed velocities. When they reach the outer bank an increase in water elevation occurs due to a sudden decrease in velocity. This creates a radial pressure gradient, due to the water surface slope, which is equal to gravitational acceleration multiplied by the water surface slope. This pressure gradient is uniform over the flow depth at a specific point along the radius (Julien 2002). As the flow near the bed experiences a smaller centrifugal force than at the surface, the radial pressure gradient eventually exceeds the centrifugal force (Figure 1.2), causing the water to be deflected towards the inner bank at the bed. This process continues, and creates what is known as a helical flow pattern. In addition, the presence of a smaller weaker counter rotating cell has been detected near the water surface at the outer bank (see Figure 1.2) in both laboratory (Rozoyskii 1965; de Vriend 1979 and 1981; Tominaga and Nagao 2000; Blanckaert and Graf 2001; Van Balen *et al.* 2009) and field studies (Bathurst *et al.* 1979; Dietrich and Smith 1983; de Vriend and Geldof 1983). This counter rotating cell has a protective effect, by keeping the core of high velocities at a distance from the bank, and thus reducing high bed shear stresses in its vicinity.

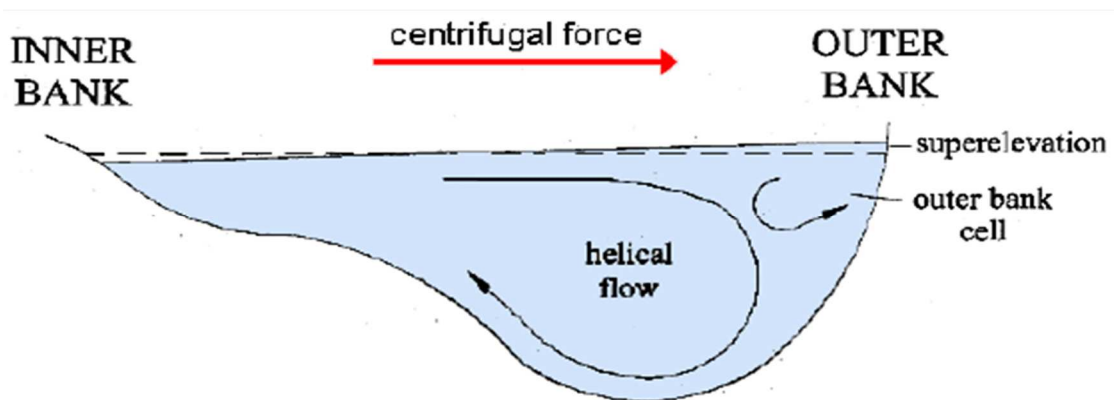


FIG 1.1 Helical flow in bend

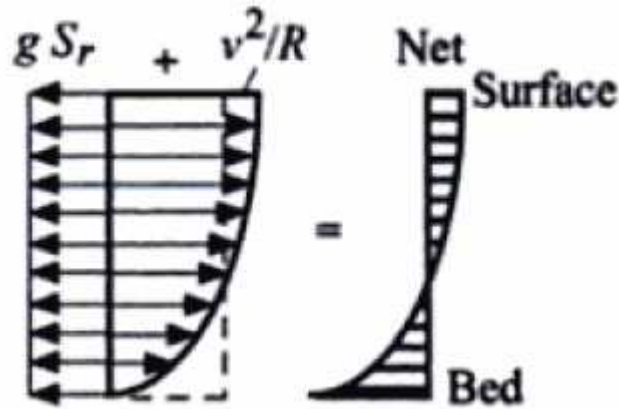


FIG 1.2 Radial Force Balance.

The net radial force is equal to the radial pressure gradient ( $gSr$ ) plus the centrifugal force ( $v^2/R$ ).  $g$  is gravitational acceleration,  $Sr$  is surface slope,  $v$  is velocity, and  $R$  is radius (Julien 2002).

## 1.5 RESEARCH STRATEGY

The simulation study for groyne placement in a river bend was done using a computational dynamic software, Ansys Fluent (v14.5). apart from the channel geometry, which was defined using AUTO CAD (2013) and then imported into Ansys, all other processes to get the required results were done under the domain of this software.

### 1.5.1 CHANNEL AND GROUYNE DESCRIPTION

TABLE 1.1 Field studies of groynes in channel bends.

REFERENCE/SITE LOCATION	GROYNE CLASSIFICATION	BEND DESCRIPTION	GROYNE PERFORMANCE
Victoria Bend, Mississippi River (Jia et al. 2009)	Repelling	Radius/Width= 1 to 3	High scour around groynes, deposition upstream
Jamuna River, Bangladesh (Mosselman et al. 2000)	Emerged, Permeable	Radius/Width=2.7	Outer bank erosion of 9 m, deposition at inner bank, outer bank stopped retreating
Red Rock Bend, Mississippi River (WST 1999)	Repelling	Radius/Width>3.5	Large scour below 7 downstream weirs, less at 2 upstream weirs

With reference to the above rivers the simulated channel section is designed with criteria of Mean Radius/Width=2.5.

The channel width is assumed a constant value of 20m, thus the mean radius is taken as 50m. The height of the channel section is 8m.

The total observation taken are 72 which consist of groynes of 4 different sizes, that is, 4m; 3.5m; 3m; 2.5m. These sizes conform to the design criteria giving by the 'Indian Standard Code IS 8408:1994', which restricts the size of groyne to 1/5 times the channel width.

Three different velocities of 2.6m/s; 2m/s and 1.4m/s were taken to observe the variation of velocity flow patterns. Since in order to find the best placement of groyne is a matter of hit and trial, six (6) different positions are taken and the best is decided among these after analysis of dependent factors.

The primary aim of this project was to protect the concave face of the river bank but due to the introduction of groyne in only this face resulted in high turbulence zone on the convex face and thus the aim had to be modified.

## **1.6 RESEARCH CONSTRAINT**

The observations taken in this study are not exhaustive in themselves and further analysis and iterations can be taken to find the best placement of groyne.

The software used for analysis Ansys Fluent (v14.5) also has some limitations-

- a) The channel boundary cannot not be defined as non-rigid or movable hence extent of scouring on the banks and bed could not be estimated.
- b) The channel bed slope could not be defined as an input.
- c) Linear measurement like arc length could not be measured precisely and attribute of another software was needed for same.

## **1.7 ORGANISATION OF DISSERTATION**

The report is subdivided into 6 chapters. *Chapter 1* states the importance of the matter and aim of the study. *Chapter 2* presents the review of the literature available on this topic. The methodology and numerical data involved in this dissertation work is discussed in *Chapter 3* and *Chapter 4* respectively. The results and the discussions are enlisted in *Chapter 5*. Finally in *Chapter 6*, conclusions and scope of future work are discussed.

## **CHAPTER 2**

### **LITERATURE REVIEW**

#### **2.1 INTRODUCTION**

This section reviews previous studies of flows around groynes installed in channel bends. This part is divided into sections dealing with experimental, field studies and numerical models. The review is organized based on fundamental flow or scour features revealed from each study.

#### **2.2 GROYNES IN A BEND – EXPERIMENTAL STUDIES**

Many early experimental/field studies on groynes in a bend (Beckstead 1978; Prezedwojski *et al.* 1995a) were case studies attempting to determine optimum groyne configurations. In recent years, experimental studies have revealed more details of flow and turbulence due to the availability of sophisticated equipment such as Acoustic Doppler Velocimeters (ADV). The USDA (2005) has developed a set of guidelines for groyne design in bends based on a thorough review of existing literature. Many challenges still exist in this area and the performance of groynes in the field has been highly variable (WST 2002).

##### **2.2.1 VELOCITY DISTRIBUTION PATTERNS**

Flow in a curved channel is subject to a helical flow induced by centrifugal forces, which leads to high shear stresses along the outer bank (Ruther and Olsen 2005; Khosronejad *et al.* 2007). Groynes attempt to disrupt this helical pattern, and shift high velocities back to the channel centreline, thereby lowering the velocity gradient along the outer bank. Kinzli and Thornton (2009) demonstrated the ability of partially-submerged weirs to do this in a series of 72 tests conducted in a rigid bed laboratory meander flume. The weirs varied in length, angle, and spacing ratio. In all the cases it was found that the maximum velocity within the recirculation zone immediately downstream of the weir was always lower than the maximum main channel centreline velocity just upstream of the weir. Abad (2008) showed that for emergent groynes the core of high stream wise velocities in the channel bend stayed inwards of the groyne tip. Ghodsian and Vaghefi (2009) also showed that T-shaped groynes aligned perpendicular to the bank were able to reduce the velocity gradient at the outer bank. High velocities are usually found around groyne tips. Kinzli and Thornton (2009) found in their series of 72 tests that the maximum velocity at the toe of bend way weirs for flatbed conditions was greater than the maximum main channel velocity.



## 2.2.2 RECIRCULATION PATTERNS

The recirculation length downstream of a groyne affects flow patterns within the embayment. This area is located between the separation point at the tip of the groyne and the reattachment point along the outer bank (Figure 2.1). The recirculation length varies depending on the level of turbulence in the flow and the intermittency of eddies being shed from the shear layer (Yossef 2005). Fazli *et al.* (2008) found that for groynes installed in a 90° bend, the recirculation length varied with groyne location along the bend. When the groynes were installed at 30° from the bend entrance, the recirculation length was shorter than when they were installed at 75° from the entrance.

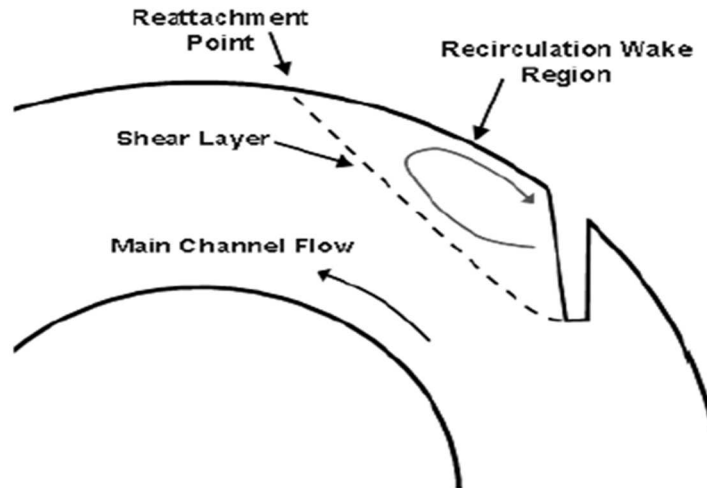


FIG.2.1 Recirculation region downstream of a groyne between the separation and reattachment point.

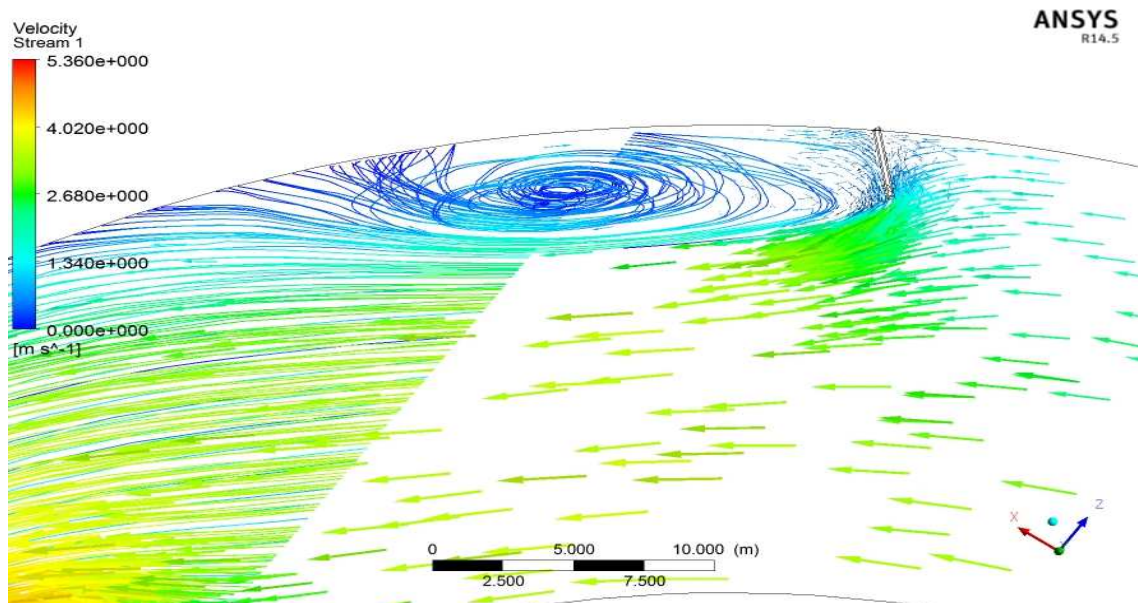


FIG.2.2 Recirculation region downstream of the groyne on concave face of bend in this study using Ansys.

## 2.3 GROYNES IN A BEND –NUMERICAL STUDIES

Numerical studies of groynes in channel bends are few compared to those done for straight channels. Nearly all former studies have used 3D RANS models, which although highly popular, face challenges when simulating complex flows involving massive separation, reattachment, and high anisotropy (Rodi 1993). In addition, they are time-averaged and do not capture the dynamic flow nature. Nevertheless, they are computationally efficient and can help reveal further details of the flow, which are difficult to measure experimentally. There are very few studies using highly-resolved models such as k-epsilon and Direct Numerical Simulation (DNS) to model groynes in a bend.

The studies presented here model flow in either a field or laboratory channel. Many of these involve bend way weirs rather than groynes, which although similar, have been optimized to improve navigation conditions rather than to mitigate bank erosion (Jia *et al.* 2001; Julien and Duncan 2003; Jia *et al.* 2005; Huang and Ng 2007; Abad *et al.* 2008; Jia *et al.* 2009).

Several of these studies are related as they present simulation results for the same flow channel using the same numerical model. This is the case for the studies of Jia *et al.* (2005), Huang and Ng (2007), and Julien and Duncan (2003), which all simulated flows around a single submerged weir in a channel meander, modelled after a laboratory channel at the U.S. Army Corps of Engineers Waterways Experimental Station. These studies used a 3D RANS model CCHE3D and validated the results with ADV data from a physical model.

### 2.3.1 HELICAL FLOW PATTERNS

Submerged groynes have been found to alter significantly the secondary helical flow patterns induced by a bend. Studies have shown that groynes create an additional secondary circulation cell of direction opposite to that of the original helical cell (Jia *et al.* 2001; Julien and Duncan 2003; Jia *et al.* 2005; Minor *et al.* 2007a; Huang and Ng 2007; Jia *et al.* 2009;). Such an example from the results of Minor *et al.*(2007a) is shown in Figure 23. The newly formed secondary cell provides the advantage of reversing the direction of velocity vectors at the toe of the outer bank, from being directed down to being directed up, which prevents excessive scour near the bank toe. In addition, the main helical secondary cell is weakened and the thalweg has relocated to the channel centre, as opposed to the outer bank.

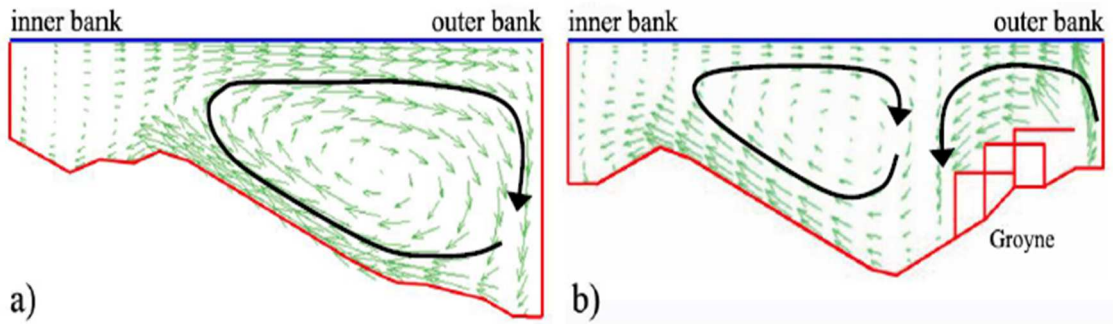


FIG.2.3 a) Channel cross-section showing secondary helical flow pattern in 90° bend without groyne and b) with groynes.

### 2.3.2 SHEAR STRESS DISTRIBUTIONS

The distribution of bed shear stress is important as sediment scour occurs when bed shear stress exceeds a critical value for particle entrainment. Although it is not the sole parameter which causes scour, the presence of groynes influences bed shear stress distribution and therefore must be investigated.

High bed shear stresses usually occur along the outer bank, due to centrifugal forces which push high velocities outwards. As investigated the effect of placing various configurations of submerged groynes in both 90° and 135° sharp bends. The groynes were configured to minimize outer bank scour. The results showed that overall the groynes had a beneficial effect on bed shear stress by moving the maximum stress inwards from the outer bank. The maximum bed shear stress often occurred near the groyne tips.

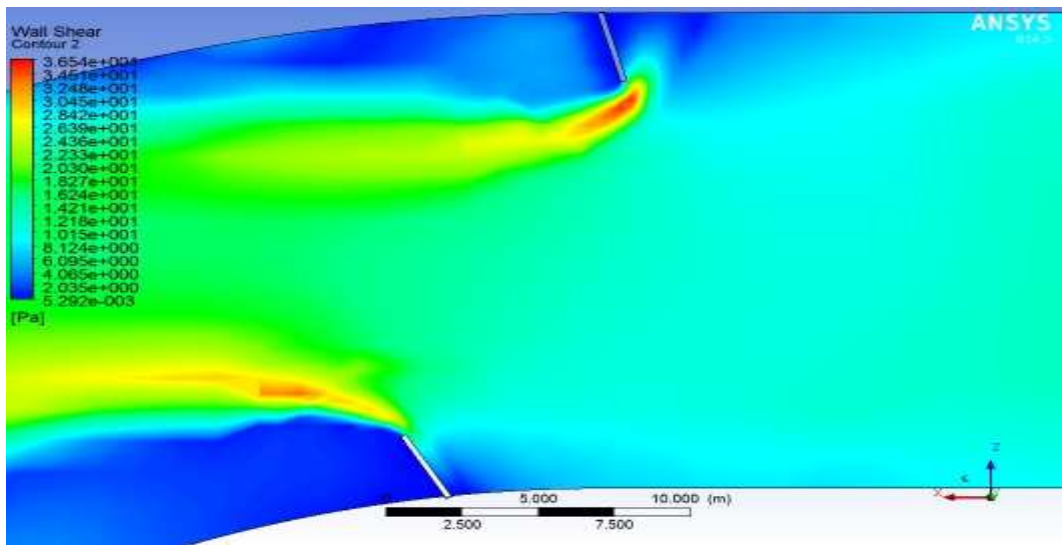


FIG.2.4 Maximum bed shear stress near the groyne tips.

### **2.3.3 VORTICITY DISTRIBUTIONS**

Vorticity distribution around groynes in a bend has received little attention. It is however important as areas of high vorticity indicate high scour. Giri *et al.* (2004) used a 2D depth-averaged model to study non-submerged spurs installed perpendicular to the bank in a meandering channel. High vertical vorticity values were present around the tips of the groynes, and their distribution patterns were observed. High turbulence intensity was also present at the tips, particularly at the first groyne. The model did not simulate scour but simulated flow for a fixed bathymetry.

Another study calculated vorticity magnitudes and vertical vorticities around a groyne field in a 90° laboratory channel bend. Vorticity magnitudes were the highest at the tips of the groynes, particularly at the tip of the first groyne. Vertical vorticities were also high at the tips of the groynes and appeared to be slightly higher at the downstream groynes, where the deepest scour was predicted.

### **2.4 NECESSITY OF LITERATURE REVIEW**

The above briefed literature review relating to studies and experiments already done in this field of research gave important insight. Since in a channel bend the complexities of flow and the factors involved are numerous thus it was important to understand which factors contribute the most and are critical for any further study.

It is important that any new research that has to be done have suitable justification for the results obtained. Since it was not possible to gather any experimental results to verify the analysis of this research, it was important to have the basics of this complex correct to get any appreciable result.

Unlike the above mentioned research, where groynes are placed only at concave face for bend protection, in my study I have tried to use groynes of opposite nature on both faces for the bend protection. This inspiration or methodology was developed after analysis of flow patterns due to a single groyne, and after many iterations it was found that this can be a probable case of research.

This research topic although based on hit and trial to get the best placement combination of groyne, selecting the best or the most appropriate case that gave satisfactory results required the study of above papers. But, in my study only the upstream effect of the convex/attracting groyne could be analysed as downstream effects were not easily quantifiable.

## **CHAPTER 3**

### **METHODOLOGY**

#### **3.1 SYNOPSIS OF SIMULATION**

The main purpose of the simulation described below is to get optimum number of observation for further analysis to be done. Though the observations taken here are not exhaustive in any respect as to find the best placement of the groynes increase in the data would also increase the accuracy of the results.

#### **3.2 CHANNEL CHARACTERISTICS**

For the following study the channel had a rectangular section for the straight reaches and a curvature for the bend sections.

The straight reaches at the beginning of the section and the end of curvature is as follows-

- a) Length=40m
- b) Width =20m(constant for the whole section)
- c) Height=8m

The mean radius of curvature of the bend is taken as 50m.

The dimensions used for simulation are with reference to a research paper.

The channel boundary and bottom are assumed to be made up of a material that is non scouring that is the boundary conditions of the channel is non mobile. This means that the effect of alluvium is not considered in flow patterns or shear stress.

#### **3.3 GROYNE CHARACTERISTICS**

The groynes used in the study are assumed to be made up of gypsum( $\text{CaSO}_4 \cdot 2\text{H}_2\text{O}$ ) with material characteristics as follows. It should be noted that since scouring effects are not considered in this study thus by using different groyne material no significant difference in results is observed.

The groynes are non-permeable in nature and they work as non-submerged groynes at every section of the channel.

Groyne used are of rectangular correction with lengths of 4m, 3.5m, 3m and 2.5m were used for making observations. The width of the groynes is taken as a constant value of 0.2m.

Since the primary objective of this simulation study is to protect the concave face of the bend, thus the groynes on this face are of repelling nature. Similarly the groynes on the convex face are attracting groynes.

### 3.4 POINTS OF OBSERVATION

In this study, groyne placement was considered at six different sections along the channel bend. The position for the initial section for the placement was decided by taking into observation the flow velocities in a channel without any groynes that is without any protection.

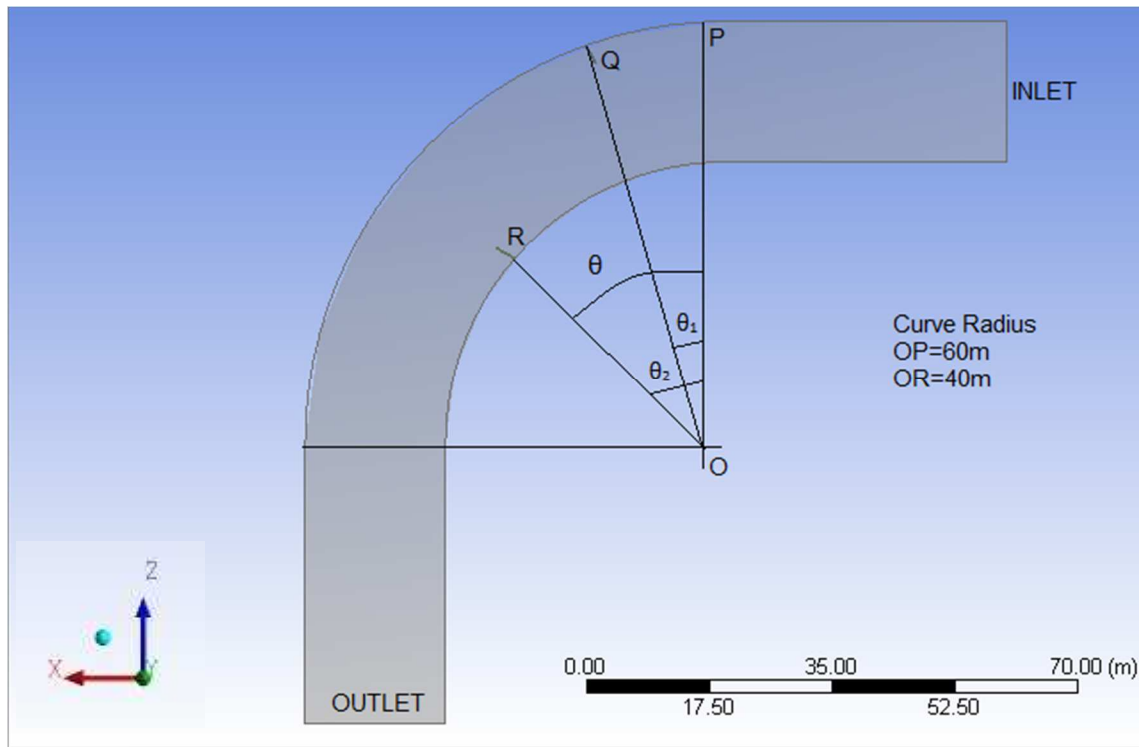


FIG 3.1 Orientation of groyne placement with respect to a fixed meridian “OP”.

OP= $R_1=60\text{m}$  AND OR= $R_2=40\text{m}$ .

Below is given the different positions of groyne placement and the groyne characteristic at these positions.

TABLE 3.1 Position of different groyne

GROYNE COMBINATION		A	B	C	D	E	F
POSITION (in degrees with respect to meridian “OP”)	CONCAVE FACE( $\theta_1$ )	$0^0$	$0^0$	$5^0$	$5^0$	$20^0$	$35^0$
	CONVEX FACE( $\theta_2$ )	$10^0$	$15^0$	$15^0$	$30^0$	$45^0$	$60^0$
INCLINATION (with respect to Y direction)	CONCAVE FACE (upstream)	15	15	15	15	30	45
	CONVEX FACE (downstream)	30	30	30	45	60	75

### 3.5 INPUT VARIABLES

Three different velocities of 2.6m/s; 2m/s;1.4m/s are used in this study for the results. These velocities are average velocities through which the computations are initialised.

The lengths of groynes used for study are 4m, 3.5m, 3m.2.5m. These groynes are non-permeable. The groynes on concave bank of channel are repelling in nature, thus pointed upstream, while those on convex bank are attracting, thus pointed downstream.

### 3.6 MEASUREMENTS

In order to determine the factors which determine the behaviour of flow pattern due to a groyne certain basic measurements are needed.

#### 3.6.1 PROTECTED LENGTH

It is the length of the concave side of the section that is protected due to the introduction of the groyne. This length varies with the size of the groyne, their placement, initial velocity of flow and upstream effect of the attracting groyne on convex face. The protected length of the convex face is not taken into consideration as before the introduction of groyne no protection was needed on this face.

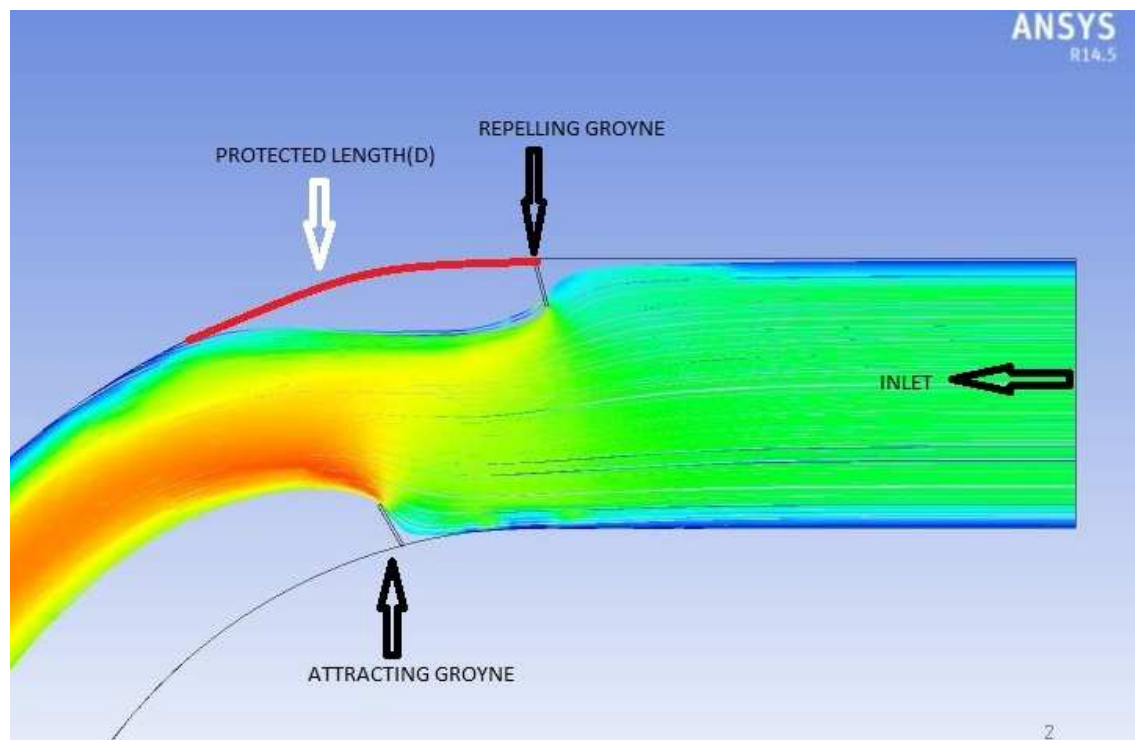


FIG 3.2 Protected length corresponding to safe bank length.

### 3.6.2 VELOCITY

There are namely three velocities that are either measured or given as input-

- a) Approach Velocity ( $V_{app}$ )-this is the input velocity that is given to initialise the simulation.
- b) Tip Velocity ( $V_{tip}$ )-this is the velocity measured near the tip of the groyne.
- c) Maximum Velocity ( $V_{max}$ )-this is the absolute or global maximum velocity in the channel.

### 3.6.3 SHEAR STRESS

The shear stress that is taken into consideration or assumed as an important factor for analysis is the maximum bed shear stress. This stress was found to be maximum in all the cases near the groyne. It is represented by the symbol  $\tau_{max}$ .

Also for regression analysis and to know the increase in stress due to introduction of groyne in channel, initial bed shear stress was also measured.it was measured at the centre line on the channel. It is represented by the symbol  $\tau_o$ .

### 3.7 SOFTWARE INPUT

The computational dynamic software used for carrying out this study is Ansys Fluent (v14.5).This software gives us the required results by simulating flow patterns in the given channel using a predefined mathematical model.

This software consists of 4 basic parts which together give the required results for a certain study. These are enumerated below. these are software prerequisites and are essential for every case of observation to be made.

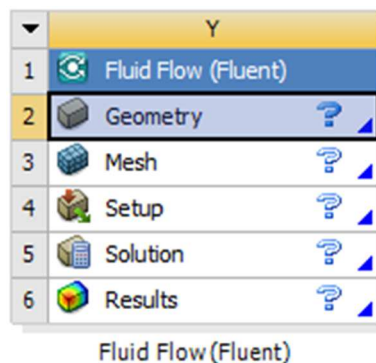


FIG.3.3. Dialog box showing basic components of Ansys Fluent.

#### 3.7.1 GEOMETRY

This is the part of the software that is used to define the channel geometry and its cross-section. It is named as 'Design Modular' in Fluent.



There are essentially 2 ways to define the geometry of the required channel-

- a) To design/draw the geometry using the tools in design modular. The section is firstly drawn in a 2-Dimensional plane of either X-Y, Y-Z or Z-X.in order to get a 3-Dimensional structure the above plane is given height or width in the direction perpendicular to the plane.

Ex- for a section drawn on X-Y plane the channel is given width or height in the Z direction to obtain a 3-D structure. This is done in Ansys Fluent using Design Modular inbuilt tools like ‘extrude’, ‘sweep’.

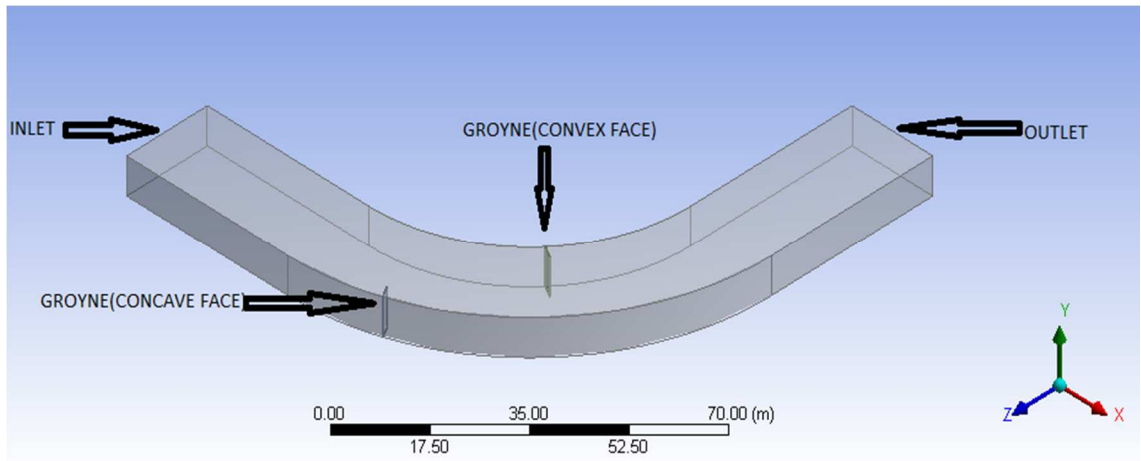


FIG.3.4 Channel Geometry as it looks in Design Modular of Ansys Fluent.

- b) The required section of channel can also be drawn in other Computer Aided Design (CAD) software like Auto CAD2013.the supported file of this geometry is then imported into the Design Modular.

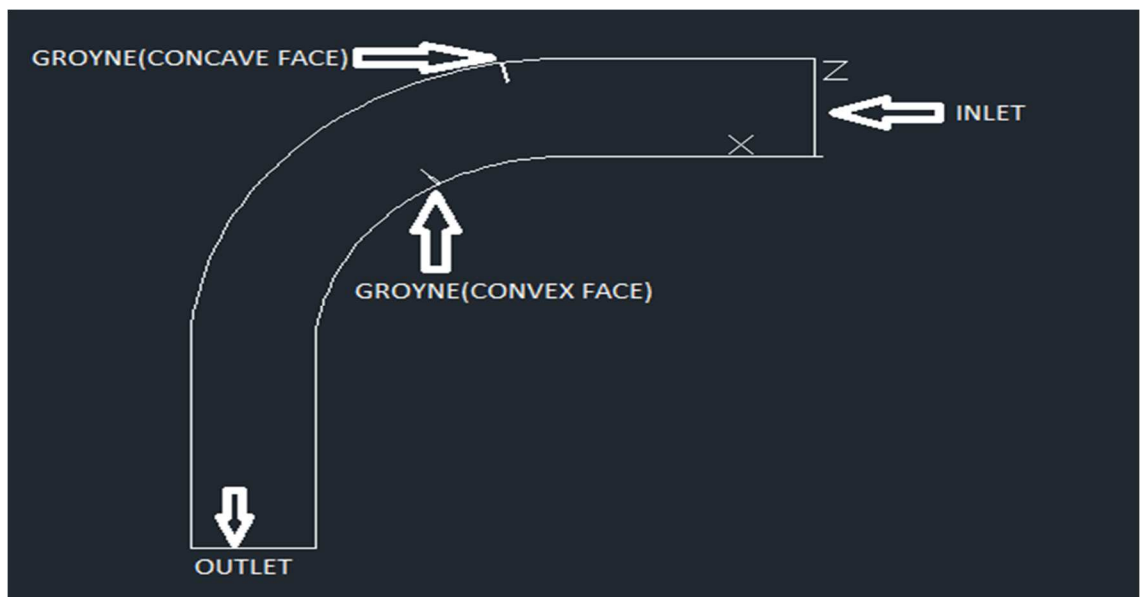


FIG.3.5 Channel Geometry as it looks in AutoCAD 2013.

Ansyes Fluent analyses on 3-D solid structures thus it is important to make sure that there are no hollow sections in the imported sturcture. Moreover the geometry that is once imported cannot be modified in the Design Modular as only the default files can be edited in it. Though it is possible to create new coordinate system or retain the same from the CAD software.

### 3.7.2 MESHING

Meshing is an integral part of the computer-aided engineering simulation process. The mesh influences the accuracy, convergence and speed of the solution. Furthermore, the time it takes to create and mesh a model is often a significant portion of the time it takes to get results from a solution. Therefore, the better and more automated the meshing, the better the solution.

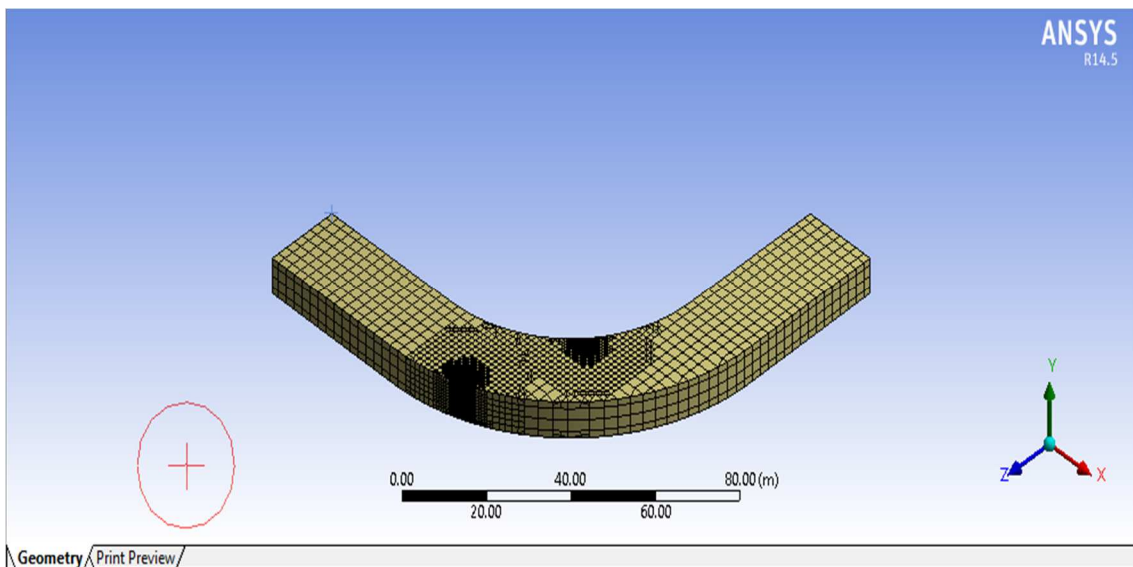


FIG.3.6 Meshing by Cut Cell Assembly method with relevance to prOPimity and curvature.

For the study undertaken the flowing meshing was used to get appropriate results-

TABLE 3.2 Meshing Components and the assigned values/method for study.

COMPONENTS	Size Function	Relevance Centre	Smoothing	Min. Size	Assembly Method
VALUES/METH OD	Proximity & curvature	Course	Medium	0.17888m	Cut Cell

It is also necessary to define the channel components, like convex face, concave face, inlet, outlet, channel bottom, groyne, and top of channel. These are also defined for the next step of setup where these are read into file so that characteristics of each of these components can be defined. Like their material and their functioning in the simulation process.

### 3.7.3 SETUP

It is the step in Ansys Fluent where the mathematical model to be used, definition of components of channel like material and their type, is done. The values needed to initialise the solution like input velocity are also provided in this step.

For the following study the mathematical model that was chosen for all the observation was ‘K-EPSILON (2eqn)’, this model gave moderately conservative results. The predefined values for this type of model are-

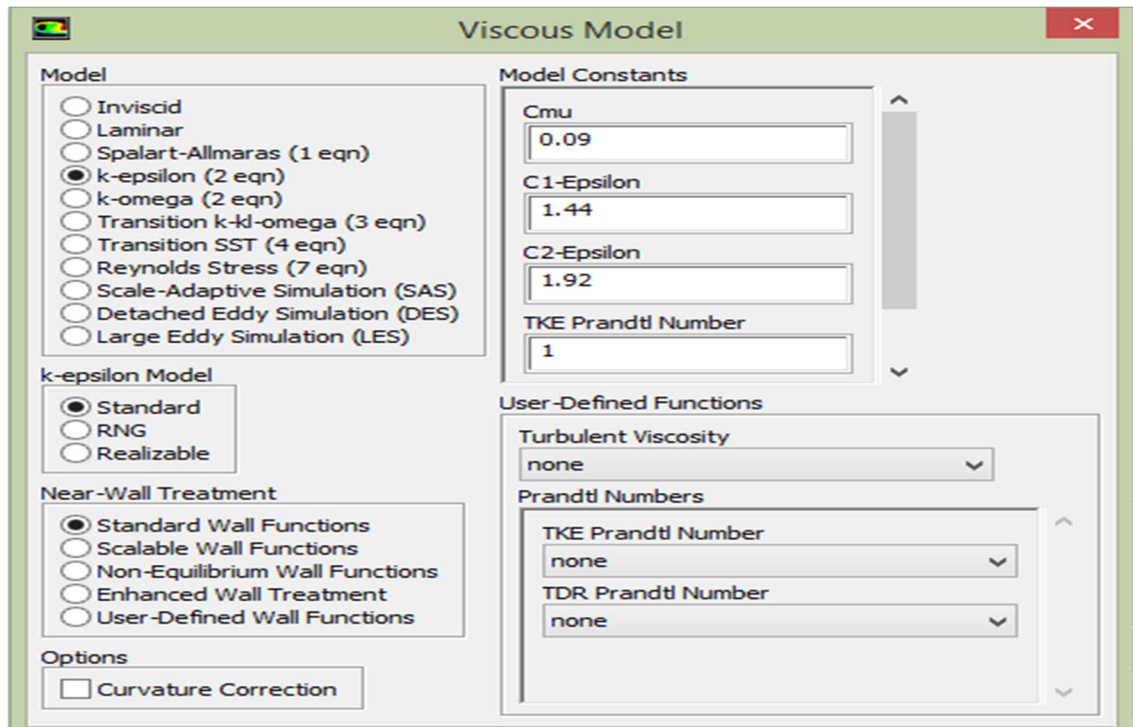


FIG 3.7 Definition of mathematical model used, k-epsilon.

This model was applied assuming a steady state condition and not transient. Gravity is defined as a constant value of  $9.81\text{m/s}^2$  in the  $-ve$  Y direction.

The boundary condition defined for the channel components is as follows-

TABLE 3.3 Boundary Condition for each case of observation.

Channel Components	Inlet	Outlet	Groyne	Top	Bottom	Boundary
Definition	Velocity Inlet	Outflow	Wall	Symmetry	Wall	Wall

### 3.7.4 SOLUTION

This is step in which the solution methods for different computations are defined and also the monitors for control. The solution is initialised with values from 'INLET' in all the observation under this study. it is necessary to initialise a solution before any calculation on the input raw data can be done.

TABLE 3.4 Solution Methods Used in this study.

Component	Pressure	Momentum	Turbulent Kinetic Energy	Turbulent Dissipation Rate	Gradient	Pressure-Velocity Coupling
Method	Standard	Second Order Upwind	Second Order Upwind	Second Order Upwind	Least Square Cell Based	Simple

For the steady state computations the number of iterations for different cases varied as in each case the solution converged at different iterations. Reporting interval that is the interval after which solution of each set are displayed can be varied accordingly. these are complex calculations and thus it is recommended to define the number of system cores at the beginning of this step to accommodate the solutions easily, without any load on the workstation.

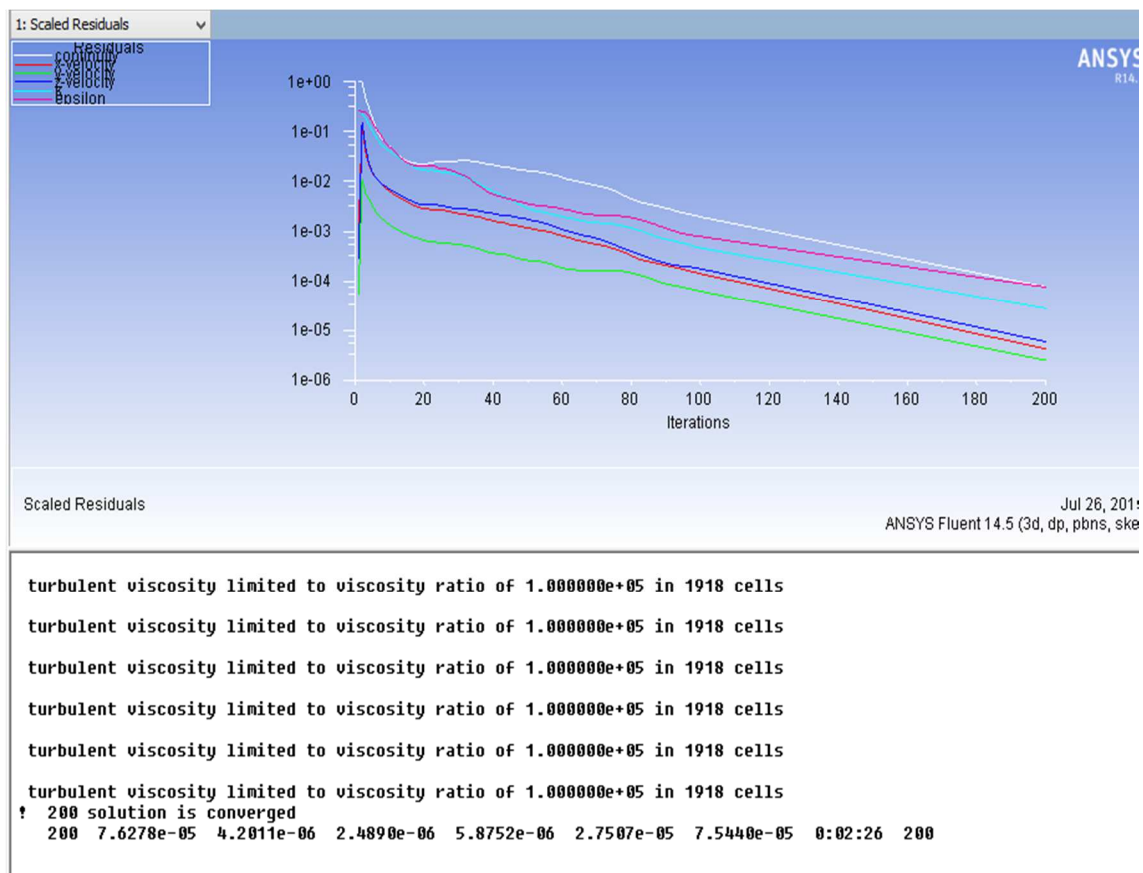


FIG.3.8 One of the case of this study where the solution converged at 200<sup>th</sup> iteration.

## CHAPTER 4

### NUMERICAL DATA

#### 4.1 INTRODUCTION

This chapter contains the data obtained from the Fluent. Total 72 cases were run for groyne of different length, position and approach velocity.

The following table contains the values of tip velocity obtained from the Fluent software. The variation of this velocity around the groyne in the vertical direction is not linear and thus the maximum velocity was found at a depth of 6m from top.

Here  $V_{app}$ = Velocity of approach to spur in m/s,  $V_{tip}$ = tip velocity at the groyne obtained numerically in m/s,  $\tau_{max}$  = maximum shear stress near the groyne in Pascal,  $\tau_o$ =initial shear stress measured at centreline in Pascal, D= protection length in m, B=width of channel in m, L=length of groyne in m.

NOTE-All the above observations are pertaining to the zone near the repelling groyne, since the aim of this study is to protect the concave face of the bend.

The different positions of groyne are abbreviated as in below table-

TABLE 4.1 Positions of groyne combination and the symbol used.

SYMBOL	CONCAVE GROYPNE(Position, orientation)	CONVEX GROYPNE(Position, orientation)	$\theta_{net} = \theta_2 - \theta_1$ (Where $\theta_1 = (l_1/R_1)$ & $\theta_2 = (l_2/R_2)$ )
A	(40m,0 <sup>0</sup> )	(45m,10 <sup>0</sup> )	0.135725
B	(40m,0 <sup>0</sup> )	(50m,15 <sup>0</sup> )	0.271465
C	(45m,5 <sup>0</sup> )	(50m,15 <sup>0</sup> )	0.168038
D	(50m,5 <sup>0</sup> )	(60m,30 <sup>0</sup> )	0.349066
E	(60m,20 <sup>0</sup> )	(70m,45 <sup>0</sup> )	0.491277
F	(70m,35 <sup>0</sup> )	(75m,60 <sup>0</sup> )	0.523598

Above  $l_1$  is the length of concave curve and  $l_2$  is the length of convex curve from the meridian "OP".

$R_1$ =radius of bend with respect to concave bank=60m

$R_2$ =radius of bend with respect to convex bank=40m

#### 4.2 EXPERIMENTAL DATA/SOFTWARE OUTPUT.

The following table gives the values of tip velocity, maximum velocity and Froude number.

TABLE 4.2 Values of tip velocity ( $V_{tip}$ ), maximum velocity ( $V_{max}$ ) Froude number and derived parameters.

Groyne	Length (L) (m)	Approach Velocity ( $V_{app}$ ) (m/s)	Tip velocity ( $V_{tip}$ )(m/s)	Maximum velocity( $V_{max}$ ) (m/s)	$V_{tip}/V_{app}$	Froude Number (Fr.)
A.1	4	2.6	4.197	5.77	1.614231	0.473762
B.1	4	2.6	3.799	5.91	1.461154	0.428835
C.1	4	2.6	3.996	5.688	1.536923	0.451072
D.1	4	2.6	3.415	5.958	1.313462	0.385489
E.1	4	2.6	3.294	6.232	1.266923	0.37183
F.1	4	2.6	3.24	6.158	1.246154	0.365734
A.1	4	2	3.228	4.42	1.614	0.36438
B.1	4	2	2.944	4.7432	1.472	0.332322
C.1	4	2	3.064	4.3644	1.532	0.345867
D.1	4	2	2.6203	4.382	1.31015	0.295782
E.1	4	2	2.526	4.641	1.263	0.285137
F.1	4	2	2.49	4.616	1.245	0.281074
A.1	4	1.4	2.28	3.07	1.628571	0.257369
B.1	4	1.4	2.072	3.11	1.48	0.233889
C.1	4	1.4	2.133	3.318	1.523571	0.240775
D.1	4	1.4	1.826	3.0346	1.304286	0.206121
E.1	4	1.4	1.758	3.085	1.255714	0.198445
F.1	4	1.4	1.737	3.09	1.240714	0.196074
A.2	3.5	2.6	4.07174	6.29108	1.566054	0.459622
B.2	3.5	2.6	3.92167	6.5288	1.508335	0.442682
C.2	3.5	2.6	3.6987	6.284	1.422577	0.417513
D.2	3.5	2.6	3.42216	6.47134	1.316215	0.386297
E.2	3.5	2.6	2.867	5.4036	1.102692	0.32363

F.2	3.5	2.6	3.11368	5.79985	1.197569	0.351475
A.2	3.5	2	3.11707	4.7048	1.558535	0.351858
B.2	3.5	2	2.967	4.467	1.4835	0.334918
C.2	3.5	2	2.836	4.09816	1.418	0.320131
D.2	3.5	2	2.55946	4.2855	1.27973	0.288914
E.2	3.5	2	2.20468	4.02135	1.10234	0.248866
F.2	3.5	2	2.3937	4.33675	1.19685	0.270203
A.2	3.5	1.4	2.17127	3.02995	1.550907	0.245095
B.2	3.5	1.4	2	2.80917	1.428571	0.225762
C.2	3.5	1.4	2.032	2.839	1.451429	0.229374
D.2	3.5	1.4	1.75546	3.026	1.2539	0.198158
E.2	3.5	1.4	1.537	2.7071	1.097857	0.173498
F.2	3.5	1.4	1.66455	2.9108	1.188964	0.187896
A.3	3	2.6	3.66513	5.17627	1.409665	0.413724
B.3	3	2.6	3.40282	5.85019	1.308777	0.384114
C.3	3	2.6	3.34325	5.05517	1.285865	0.377389
D.3	3	2.6	3.19146	5.14811	1.227485	0.360255
E.3	3	2.6	3.01	5.30612	1.157692	0.339772
F.3	3	2.6	2.94745	5.3604	1.133635	0.332711
A.3	3	2	2.81094	3.88892	1.40547	0.317302
B.3	3	2	2.61142	3.81518	1.30571	0.29478
C.3	3	2	2.55307	3.74323	1.276535	0.288193
D.3	3	2	2.44369	3.7949	1.221845	0.275846
E.3	3	2	2.30987	3.96262	1.154935	0.26074
F.3	3	2	2.26087	4.00911	1.130435	0.255209
A.3	3	1.4	1.96464	2.6552	1.403314	0.221771
B.3	3	1.4	1.82595	2.82509	1.30425	0.206115
C.3	3	1.4	1.7765	2.74994	1.268929	0.200533
D.3	3	1.4	1.69529	2.58087	1.210921	0.191366
E.3	3	1.4	1.59955	2.65546	1.142536	0.180559

F.3	3	1.4	1.57718	2.70684	1.126557	0.178034
A.4	2.5	2.6	3.5417	4.6448	1.362192	0.399791
B.4	2.5	2.6	3.35171	4.8067	1.289119	0.378344
C.4	2.5	2.6	3.33169	4.77915	1.281419	0.376084
D.4	2.5	2.6	3.05075	4.4565	1.173365	0.344372
E.4	2.5	2.6	2.7884	4.82631	1.072462	0.314757
F.4	2.5	2.6	2.81623	4.90383	1.083165	0.317899
A.4	2.5	2	2.72248	3.55783	1.36124	0.307316
B.4	2.5	2	2.56493	3.71795	1.282465	0.289532
C.4	2.5	2	2.52655	3.53967	1.263275	0.285199
D.4	2.5	2	2.31846	3.52413	1.15923	0.26171
E.4	2.5	2	2.134	3.62402	1.067	0.240888
F.4	2.5	2	2.15706	3.6674	1.07853	0.243491
A.4	2.5	1.4	1.87234	2.48306	1.337386	0.211352
B.4	2.5	1.4	1.77287	2.46818	1.266336	0.200123
C.4	2.5	1.4	1.73457	2.45808	1.238979	0.1958
D.4	2.5	1.4	1.61323	2.35002	1.152307	0.182103
E.4	2.5	1.4	1.4833	2.471	1.0595	0.167436
F.4	2.5	1.4	1.49553	2.51785	1.068236	0.168817

Using the above values two dimensionless factor are defined that are-

a)  $V_{tip}/V_{app}$ .

b) Froude Number (Fr.).

These will help in better understanding of relationship between factors and their interdependence.

TABLE 4.3 Values of protected length (D) and groyne length (L)

Groyne	Length(L) (m)	$V_{app}$ (m/s)	Protected Length(D)(m)	D/L	L/B
A.1	4	2.6	24.22	6.055	0.2
B.1	4	2.6	25.74	6.435	0.2
C.1	4	2.6	21.76	5.44	0.2
D.1	4	2.6	27.8	6.95	0.2



E.1	4	2.6	34.88	8.72	0.2
F.1	4	2.6	36.88	9.22	0.2
A.1	4	2	20.9	5.225	0.2
B.1	4	2	24.02	6.005	0.2
C.1	4	2	19.76	4.94	0.2
D.1	4	2	26.92	6.73	0.2
E.1	4	2	35	8.75	0.2
F.1	4	2	36.18	9.045	0.2
A.1	4	1.4	19.76	4.94	0.2
B.1	4	1.4	23.76	5.94	0.2
C.1	4	1.4	18.62	4.655	0.2
D.1	4	1.4	25.48	6.37	0.2
E.1	4	1.4	34.46	8.615	0.2
F.1	4	1.4	35.64	8.91	0.2
A.2	3.5	2.6	23.24	6.64	0.175
B.2	3.5	2.6	26.5	7.571429	0.175
C.2	3.5	2.6	21.3	6.085714	0.175
D.2	3.5	2.6	33.08	9.451429	0.175
E.2	3.5	2.6	28.88	8.251429	0.175
F.2	3.5	2.6	39.2	11.2	0.175
A.2	3.5	2	23.1	6.6	0.175
B.2	3.5	2	25.56	7.302857	0.175
C.2	3.5	2	21.1	6.028571	0.175
D.2	3.5	2	32.56	9.302857	0.175
E.2	3.5	2	30.1	8.6	0.175
F.2	3.5	2	38.4	10.97143	0.175
A.2	3.5	1.4	22.96	6.56	0.175
B.2	3.5	1.4	24.52	7.005714	0.175
C.2	3.5	1.4	19.88	5.68	0.175
D.2	3.5	1.4	31.96	9.131429	0.175

E.2	3.5	1.4	28.08	8.022857	0.175
F.2	3.5	1.4	37.2	10.62857	0.175
A.3	3	2.6	21.82	7.273333	0.15
B.3	3	2.6	25.28	8.426667	0.15
C.3	3	2.6	21.82	7.273333	0.15
D.3	3	2.6	28.32	9.44	0.15
E.3	3	2.6	30.78	10.26	0.15
F.3	3	2.6	35.36	11.78667	0.15
A.3	3	2	21.28	7.093333	0.15
B.3	3	2	24.84	8.28	0.15
C.3	3	2	21.58	7.193333	0.15
D.3	3	2	28.74	9.58	0.15
E.3	3	2	32.46	10.82	0.15
F.3	3	2	34.88	11.62667	0.15
A.3	3	1.4	20.5	6.833333	0.15
B.3	3	1.4	24.34	8.113333	0.15
C.3	3	1.4	21.4	7.133333	0.15
D.3	3	1.4	30.26	10.08667	0.15
E.3	3	1.4	33.88	11.29333	0.15
F.3	3	1.4	32.5	10.83333	0.15
A.4	2.5	2.6	23.6	9.44	0.125
B.4	2.5	2.6	25.38	10.152	0.125
C.4	2.5	2.6	21.6	8.64	0.125
D.4	2.5	2.6	30.12	12.048	0.125
E.4	2.5	2.6	28.62	11.448	0.125
F.4	2.5	2.6	35.82	14.328	0.125
A.4	2.5	2	21.3	8.52	0.125
B.4	2.5	2	24.42	9.768	0.125
C.4	2.5	2	21.34	8.536	0.125
D.4	2.5	2	29.68	11.872	0.125

E.4	2.5	2	33.7	13.48	0.125
F.4	2.5	2	34.3	13.72	0.125
A.4	2.5	1.4	25.12	10.048	0.125
B.4	2.5	1.4	24.26	9.704	0.125
C.4	2.5	1.4	21.16	8.464	0.125
D.4	2.5	1.4	28.66	11.464	0.125
E.4	2.5	1.4	32.98	13.192	0.125
F.4	2.5	1.4	33.7	13.48	0.125

Using the above values two dimensionless factor are defined that are-

- a) D/L.
- b) L/B.

The following table contains the values of maximum bed shear stress  $\tau_{\max}$  and initial shear stress (undisturbed)  $\tau_0$  in Pascal at the bottom of the bed obtained numerically for all the cases near the groyne. The maximum shear stress was observed near the groyne.

Here  $\tau_{\max}$  = maximum bed shear stress near the groyne,  $\tau_0$ = initial shear stress at the channel bed on the centreline before the effect of spur,  $\tau_{\max}/\tau_0$ = shear stress amplification.

TABLE 4.4 Values of maximum shear stress and initial shear stress (undisturbed) and derived factors.

Groyne	Length	$V_{\text{app}}$	$(\tau_{\max})_{\text{max}}$ shear stress	$(\tau_0)_{\text{initial}}$ shear	$(\tau_{\max})/(\tau_0)$
A.1	4	2.6	47.7865	14.94	3.198561
B.1	4	2.6	41.6848	14.94	2.790147
C.1	4	2.6	43.7085	14.94	2.925602
D.1	4	2.6	33.5617	14.94	2.246432
E.1	4	2.6	31.308	14.94	2.095582
F.1	4	2.6	30.79	14.94	2.06091
A.1	4	2	29.8179	10.8525	2.74756
B.1	4	2	26.4098	10.8525	2.433522
C.1	4	2	27.2015	10.8525	2.506473

D.1	4	2	20.6197	10.8525	1.899995
E.1	4	2	19.47	10.8525	1.794057
F.1	4	2	19.01	10.8525	1.75167
A.1	4	1.4	15.6117	7.045	2.215997
B.1	4	1.4	13.45	7.045	1.909155
C.1	4	1.4	13.9084	7.045	1.974223
D.1	4	1.4	10.5447	7.045	1.496764
E.1	4	1.4	10.0245	7.045	1.422924
F.1	4	1.4	9.67	7.045	1.372605
A.2	3.5	2.6	45.31	14.94	3.032798
B.2	3.5	2.6	40.268	14.94	2.695315
C.2	3.5	2.6	41.0463	14.94	2.74741
D.2	3.5	2.6	35.4109	14.94	2.370207
E.2	3.5	2.6	26.7699	14.94	1.791827
F.2	3.5	2.6	28.1934	14.94	1.887108
A.2	3.5	2	28.0346	10.8525	2.583239
B.2	3.5	2	24.4929	10.8525	2.25689
C.2	3.5	2	25.2959	10.8525	2.330882
D.2	3.5	2	19.6605	10.8525	1.81161
E.2	3.5	2	16.3012	10.8525	1.502069
F.2	3.5	2	17.3839	10.8525	1.601834
A.2	3.5	1.4	14.5948	7.045	2.071654
B.2	3.5	1.4	11.0531	7.045	1.568928
C.2	3.5	1.4	12.8594	7.045	1.825323
D.2	3.5	1.4	10.224	7.045	1.451242
E.2	3.5	1.4	8.54896	7.045	1.213479
F.2	3.5	1.4	8.9067	7.045	1.264258
A.3	3	2.6	36.5147	14.94	2.44409
B.3	3	2.6	32.0225	14.94	2.143407
C.3	3	2.6	34.6539	14.94	2.319538

D.3	3	2.6	27.1632	14.94	1.818153
E.3	3	2.6	23.9616	14.94	1.603855
F.3	3	2.6	26.1368	14.94	1.749451
A.3	3	2	22.276	10.8525	2.052615
B.3	3	2	19.6725	10.8525	1.812716
C.3	3	2	21.343	10.8525	1.966644
D.3	3	2	16.654	10.8525	1.534577
E.3	3	2	14.9196	10.8525	1.374762
F.3	3	2	15.9884	10.8525	1.473246
A.3	3	1.4	11.4606	7.045	1.626771
B.3	3	1.4	10.1253	7.045	1.437232
C.3	3	1.4	10.8271	7.045	1.536849
D.3	3	1.4	8.4693	7.045	1.202172
E.3	3	1.4	7.76414	7.045	1.102078
F.3	3	1.4	8.1246	7.045	1.153243
A.4	2.5	2.6	30.7085	14.94	2.055455
B.4	2.5	2.6	22.7615	14.94	1.523527
C.4	2.5	2.6	23.2868	14.94	1.558688
D.4	2.5	2.6	20.5309	14.94	1.374224
E.4	2.5	2.6	22.4329	14.94	1.501533
F.4	2.5	2.6	23.3385	14.94	1.562149
A.4	2.5	2	18.8628	10.8525	1.738106
B.4	2.5	2	17.2601	10.8525	1.590426
C.4	2.5	2	17.9524	10.8525	1.654218
D.4	2.5	2	12.7547	10.8525	1.175278
E.4	2.5	2	13.9173	10.8525	1.282405
F.4	2.5	2	14.3399	10.8525	1.321345
A.4	2.5	1.4	9.7983	7.045	1.390816
B.4	2.5	1.4	8.93729	7.045	1.2686
C.4	2.5	1.4	8.9838	7.045	1.275202

D.4	2.5	1.4	6.522	7.045	0.925763
E.4	2.5	1.4	7.17891	7.045	1.019008
F.4	2.5	1.4	7.28554	7.045	1.034143

### 4.3 PLOTS OBTAINED FROM ANSYS FLUENT (CFD –POST)

The results below are for some of the positions of groynes in the channel. All the plots are for velocity of 2.6m/s. The flow is taking place from right to left.

The groyne length for each case shown here is 3m and width 0.2m.

#### 4.3.1 STREAMLINES

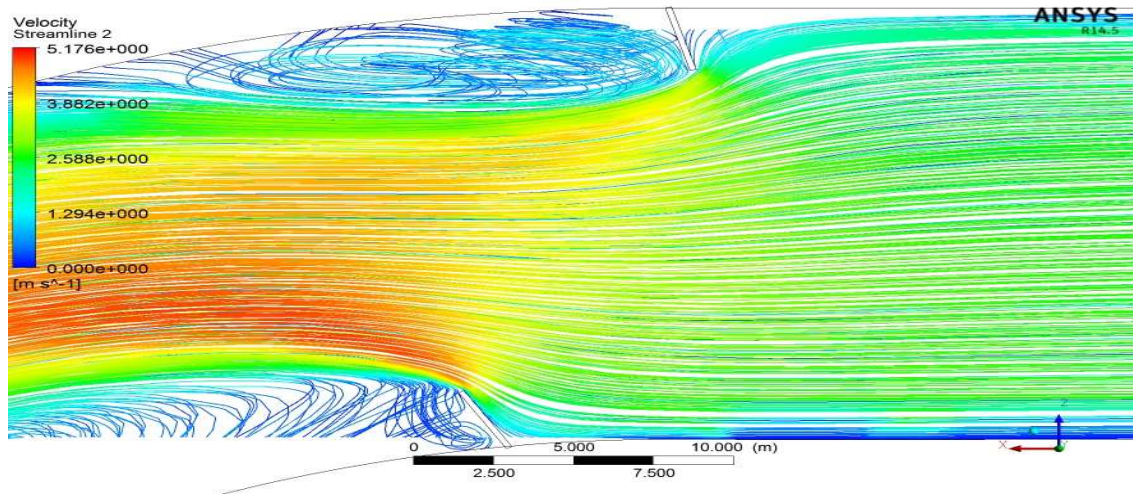


FIG.4.1 Streamlines for groyne position “A” that is attracting at  $0^{\circ}$  and repelling at  $10^{\circ}$ , with respect to decided meridian “OP”.

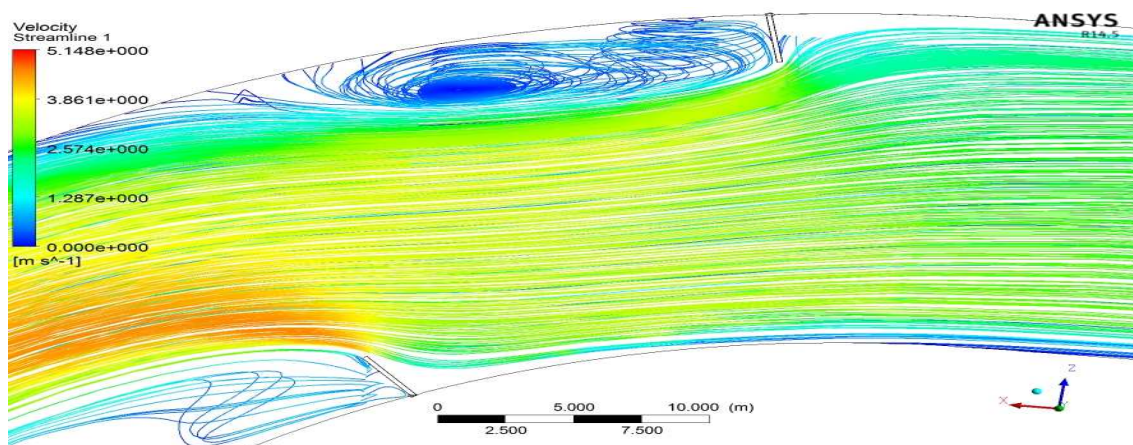


FIG.4.2 Streamlines for groyne position “D” that is attracting at  $5^{\circ}$  and repelling at  $30^{\circ}$ , with respect to decided meridian “OP”.

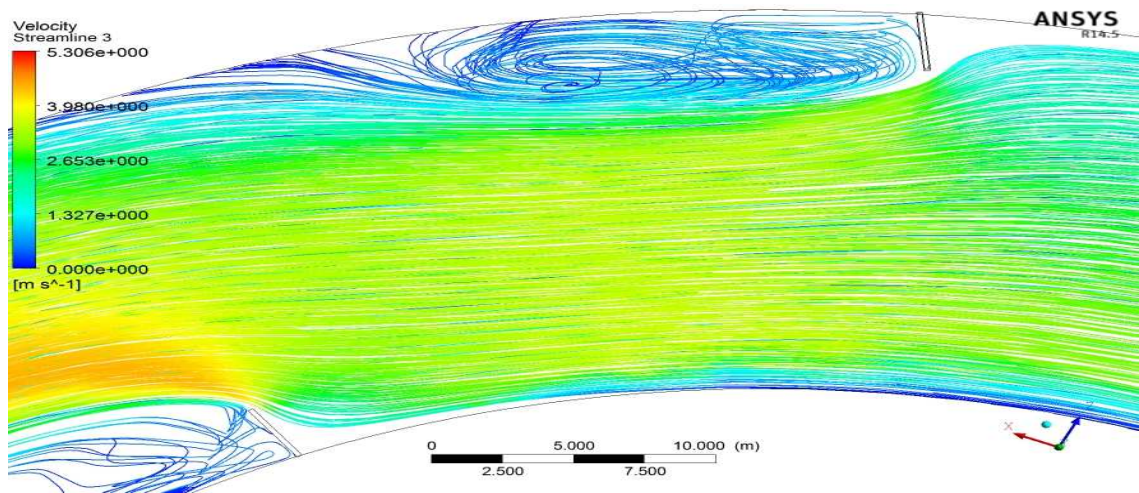


FIG.4.3 Streamlines for groyne position “E” that is attracting at  $20^{\circ}$  and repelling at  $45^{\circ}$ , with respect to decided meridian “OP”.

#### 4.3.2 VELOCITY VECTORS

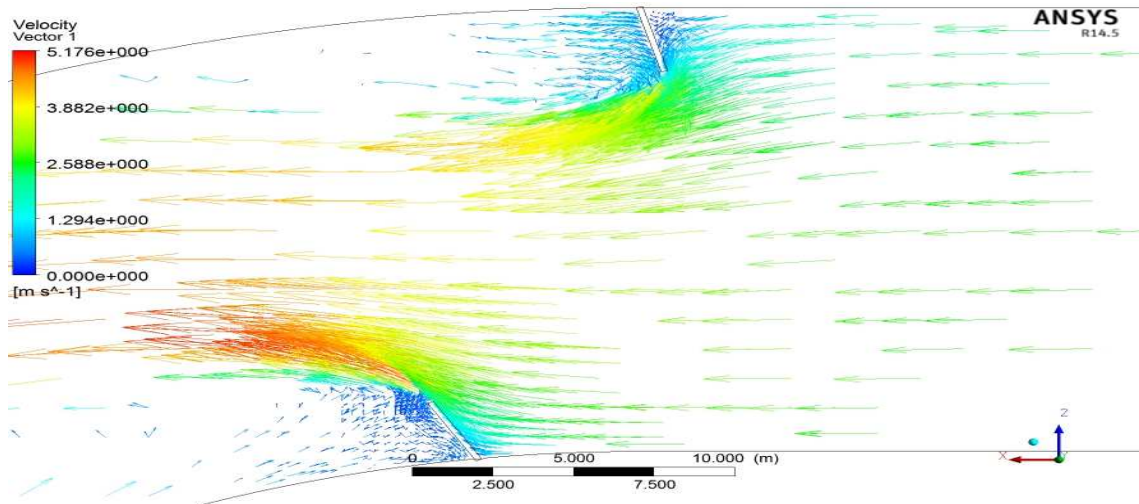


FIG.4.4 Velocity vectors for groyne position “A” that is attracting at  $0^{\circ}$  and repelling at  $10^{\circ}$ , with respect to decided meridian “OP”.



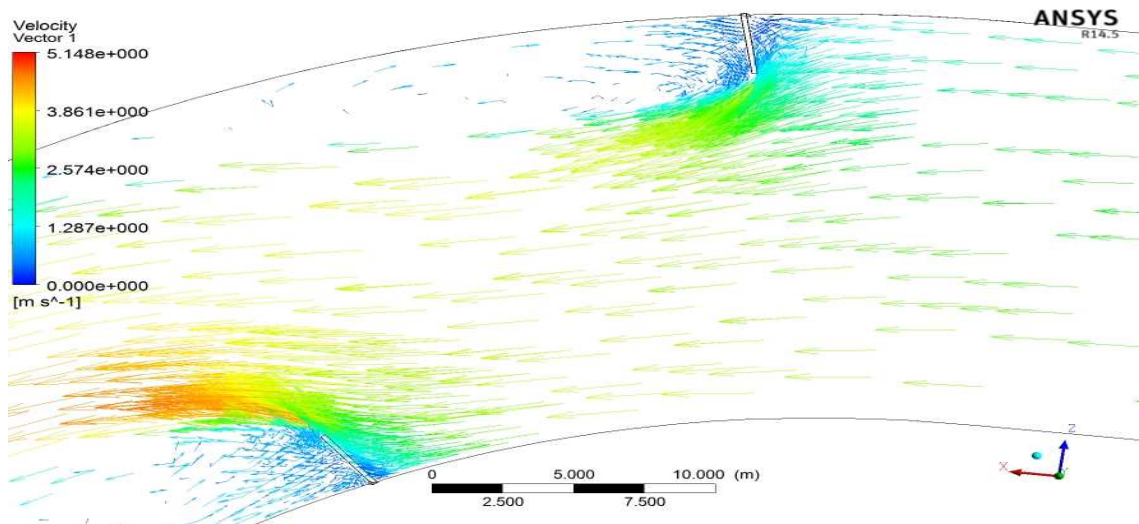


FIG.4.5 Velocity vectors for groyne position “D” that is attracting at  $5^{\circ}$  and repelling at  $30^{\circ}$ , with respect to decided meridian “OP”.

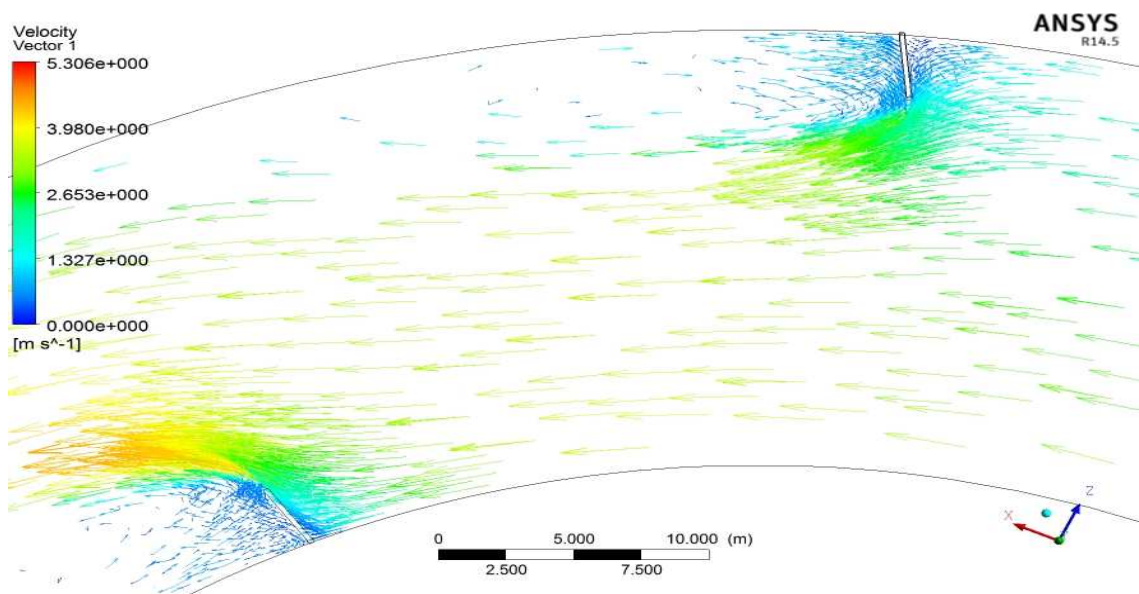


FIG.4.6 Velocity vectors for groyne position “E” that is attracting at  $20^{\circ}$  and repelling at  $45^{\circ}$ , with respect to decided meridian “OP”.



### 4.3.3 CONTOURS OF VELOCITY IN MODEL SPACE.

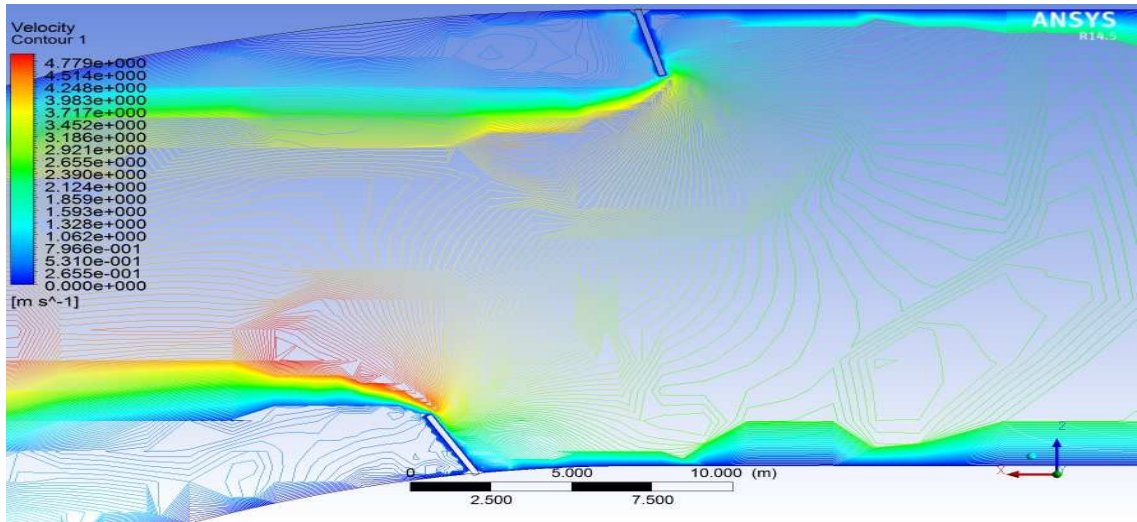


FIG.4.7 Velocity contours for groyne position “A” that is attracting at  $0^0$  and repelling at  $10^0$ , with respect to decided meridian “OP”.

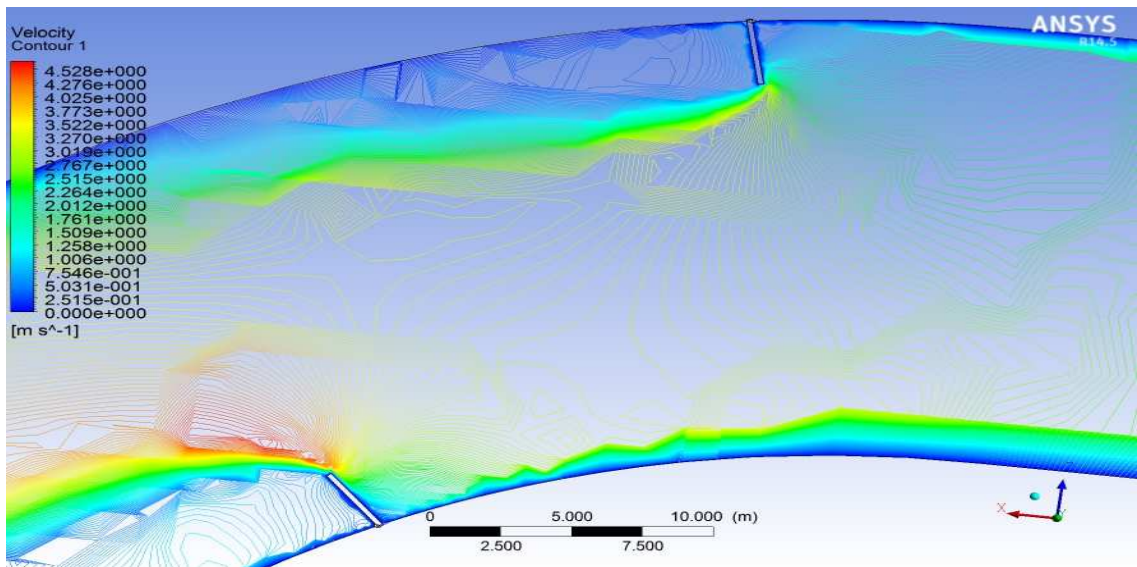


FIG.4.8 Velocity contours for groyne position “D” that is attracting at  $5^0$  and repelling at  $30^0$ , with respect to decided meridian “OP”.

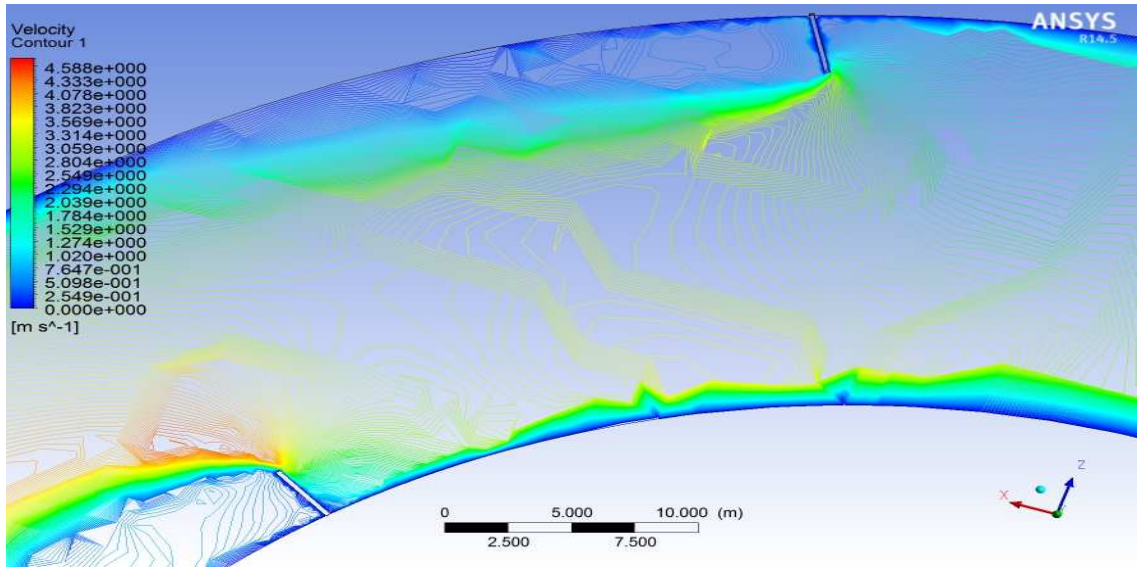


FIG.4.9 Velocity contours for groyne position “E” that is attracting at  $20^0$  and repelling at  $45^0$ , with respect to decided meridian “OP”.

#### 4.3.4 CONTOURS OF BED SHEAR STRESS

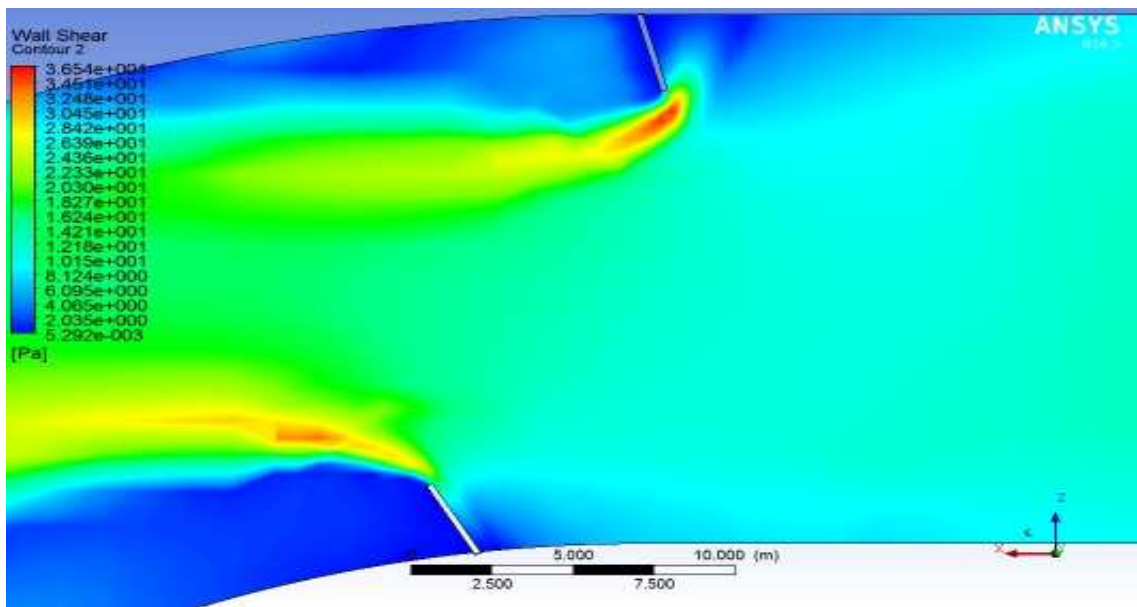


FIG.4.10 Bed shear stress contours for groyne position “A” that is attracting at  $0^0$  and repelling at  $10^0$ , with respect to decided meridian “OP”

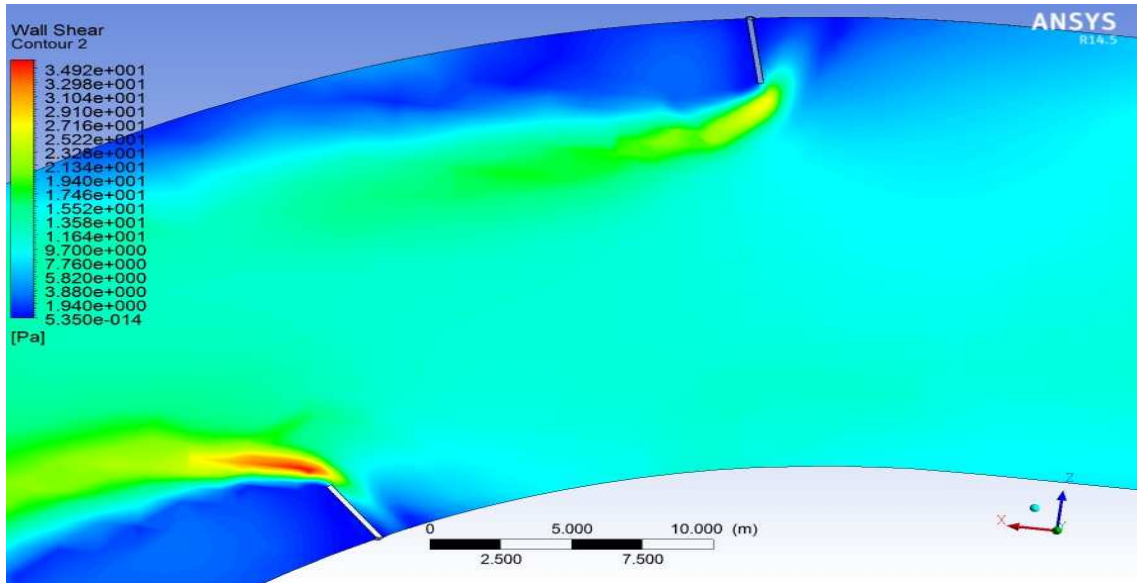


FIG.4.11 Bed shear stress contours for groyne position “D” that is attracting at  $5^{\circ}$  and repelling at  $30^{\circ}$ , with respect to decided meridian “OP”

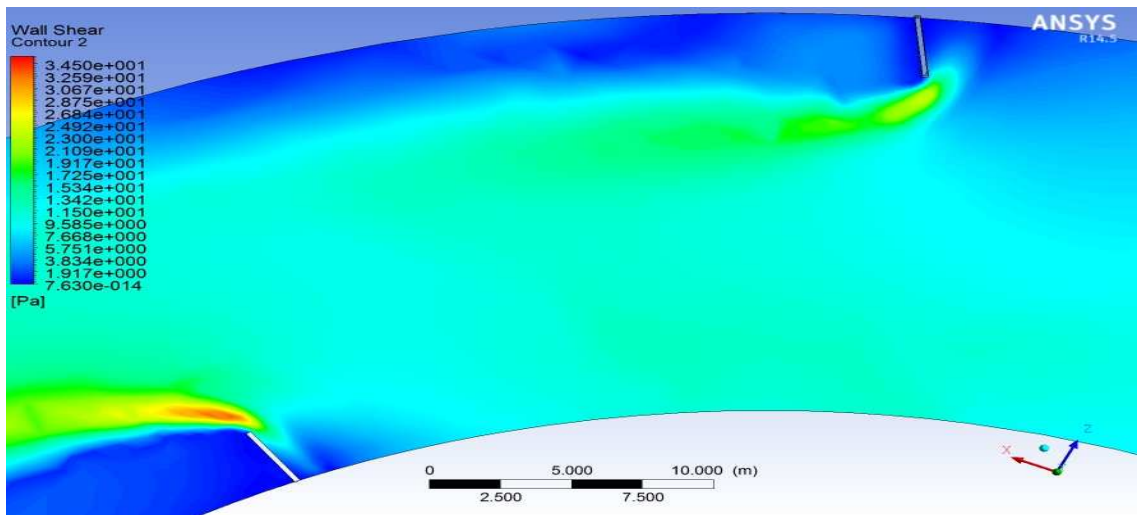


FIG.4.12 Bed shear stress contours for groyne position “E” that is attracting at  $20^{\circ}$  and repelling at  $45^{\circ}$ , with respect to decided meridian “OP”.

## CHAPTER 5

### RESULTS AND ANALYSIS

#### 5.1 INTRODUCTION

The aim of this study was to find the best placement of groynes in a channel bend. There are a number of factors that influence the complex flow which takes place in a channel bend. Though introduction structures like groynes, spurs or guide banks help train the river, they simultaneously make the analysis of the river regime more difficult. Thus the following analysis in this study is regression based, since it is not possible to predict all the factors affecting the flow and how much is their contribution.

#### 5.2 FACTORS AFFECTING THE FLOW IN A RIVER BEND.

The major factors that can be thought to predict the flow around spurs in a bend are namely-

- a) Maximum Shear Stress.
- b) Velocity near the tip of the groyne or Tip velocity.
- c) Froude Number
- d) Protection length, that is the length of bank protected due to the introduction of groyne.
- e) Groyne Length.
- f) Radius of Bend.
- g) Absolute maximum velocity

Thus from the various observation on different groyne size and their position, an appreciable relation between different factors was found.

#### 5.3 REGRESSION ANALYSIS

In this analysis empirical relation between the different factors that influence the flow is found using a series of multiple linear regressions.

The dimensionless factor used are-

- a)  $\tau_{\max}/\tau_0$
- b)  $V_{\text{tip}}/V_{\text{app}}$
- c)  $\theta_{\text{net}}$
- d)  $L/B$
- e) Froude Number.

Note- The radius of bend and the width of groyne maybe also a factor but they are assumed constant for this study.

Mean radius of bend(R) =50m; Width of channel (B) =20m

### 5.3.1 REGRESSION FOR PROTECTED LENGTH.

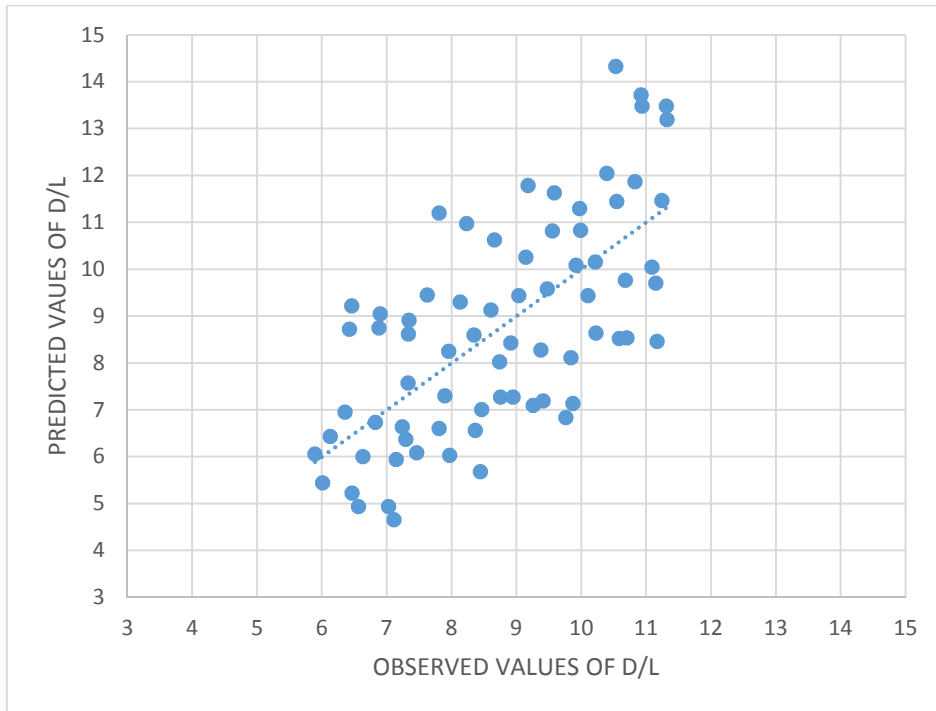
i) In this analysis the dependent variable is D/L and independent variable are Froude no.(Fr) and L/B.

SUMMARY OUTPUT						
<i>Regression Statistics</i>						
Multiple R	0.678441					
R Square	0.460282					
Adjusted R Square	0.444638					
Standard Error	1.740541					
Observations	72					
<i>ANOVA</i>						
	<i>df</i>	<i>SS</i>	<i>MS</i>	<i>F</i>	<i>Significance F</i>	
Regression	2	178.2681	89.13407	29.42222	5.75E-10	
Residual	69	209.0342	3.029481			
Total	71	387.3024				
	<i>Coefficients</i>	<i>Standard Error</i>	<i>t Stat</i>	<i>P-value</i>	<i>Lower 95%</i>	<i>Upper 95%</i>
Intercept	18.5644	1.306352	14.21086	3.54E-22	15.9583	21.1705
Fr.	-5.23117	2.589623	-2.02005	0.047263	-10.3973	-0.06501
L/B	-50.979	7.521598	-6.77769	3.36E-09	-65.9842	-35.9739

SUMMARY OUTPUT						
<i>Regression Statistics</i>						
Multiple R	0.678441					
R Square	0.460282					
Adjusted R Square	0.444638					
Standard Error	1.740541					
Observations	72					
<i>ANOVA</i>						
	<i>df</i>	<i>SS</i>	<i>MS</i>	<i>F</i>	<i>Significance F</i>	
Regression	2	178.2681	89.13407	29.42222	5.75E-10	
Residual	69	209.0342	3.029481			
Total	71	387.3024				
	<i>Coefficients</i>	<i>Standard Error</i>	<i>t Stat</i>	<i>P-value</i>	<i>Lower 95%</i>	<i>Upper 95%</i>
Intercept	18.5644	1.306352	14.21086	3.54E-22	15.9583	21.1705

Fr.	-5.23117	2.589623	-2.02005	0.047263	-10.3973	-0.065
L/B	-50.979	7.521598	-6.77769	3.36E-09	-65.9842	-35.97

For the above analysis the correlation coefficient R comes out to be 0.678 which shows that the relation between variables is poor and thus there are other factors playing a role and influencing D/L that is the Protected Length (D).



The scatter plot also shows clearly that the developed regression equation does not hold well with the results of this study.

Thus further analysis is needed to get the factors influencing the Protected Length.

ii) In this analysis the dependent variable is D/L and independent variable are Froude no.(Fr) , L/B and  $\theta_{net}$ .

<i>Regression Statistics</i>						
Multiple R	0.963959					
R Square	0.929217					
Adjusted R Square	0.926094					
Standard Error	0.14288					
Observations	72					
ANOVA						
	<i>df</i>	<i>SS</i>	<i>MS</i>	<i>F</i>	<i>Significance F</i>	

Regression	3	18.2238	6.07459 9	297.561 6	5.07E-39	
Residual	68	1.388192	0.02041 5			
Total	71	19.61199				
	<i>Coefficient</i>	<i>Standard</i>	<i>t Stat</i>	<i>P-value</i>	<i>Lower 95%</i>	<i>Upper</i>
	<i>s</i>	<i>Error</i>				<i>95%</i>
Intercept	-0.25559	0.119962	-2.13056	0.03674 5	-0.49497	-0.01621
Fr.	4.042865	0.226037	17.8858 8	2.06E-27	3.591815	4.49391 4
L/B	7.744124	0.619376	12.5031 1	2.72E-19	6.508179	8.98006 9
θ	-1.16856	0.121182	-9.64301	2.36E-14	-1.41038	-0.92675

SUMMARY OUTPUT

*Regression Statistics*

Multiple R	0.959057
R Square	0.919791
Adjusted R Square	0.916252
Standard Error	0.675901
Observations	72

ANOVA

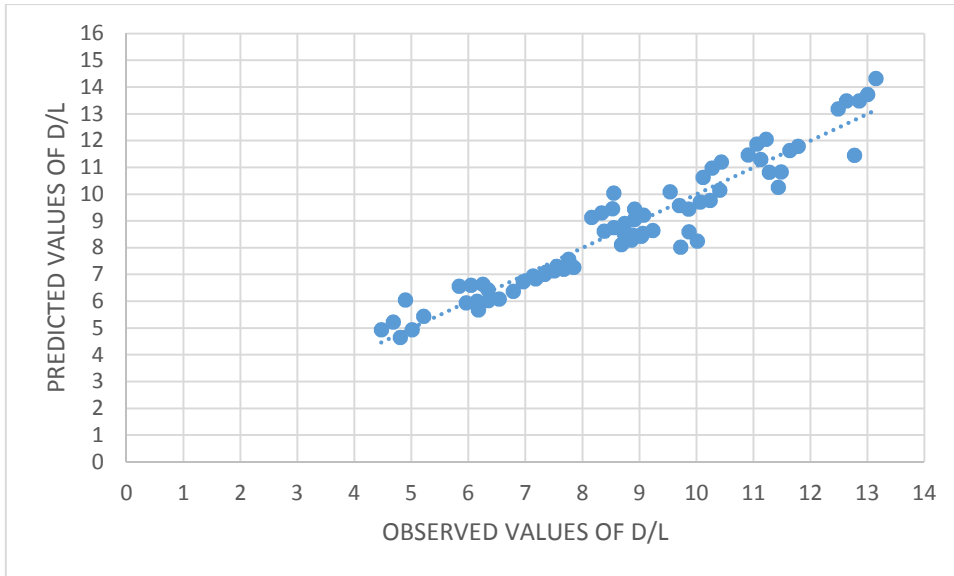
	<i>df</i>	<i>SS</i>	<i>MS</i>	<i>F</i>	<i>Significance F</i>
Regression	3	356.2371	118.7457	259.927	3.54E-37
Residual	68	31.06528	0.456842		
Total	71	387.3024			

	<i>Coefficients</i>	<i>Standard Error</i>	<i>t Stat</i>	<i>P-value</i>	<i>Lower 95%</i>	<i>Upper 95%</i>
Intercept	13.54406	0.56749	23.86662	9.08E-35	12.41165	14.67647
Fr.	1.941994	1.069281	1.816168	0.073753	-0.19172	4.075711
L/B	-55.5449	2.929996	-18.9573	7.55E-29	-61.3916	-49.6981
θ	11.31463	0.57326	19.73735	7.38E-30	10.17071	12.45856

For the above analysis the correlation coefficient R comes out to be 0.959 which shows that the relation between variables is good and a regression equation can be developed. The value of adjusted R square comes out to be 0.92 which means 92% of the values fit the equation. The value of significance F is less than 0.05 which means the equation is ok. Also all the P-values are less than 0.05 which means the independent variables used are good to be used.

Regression equation-  $D/L = 13.54406 + 1.941994Fr - 55.5449L/B + 11.31463\theta$





The scatter plot between predicted and observed values also shows a linear relationship, thus the regression equation can be used to predict the protected length for any case.

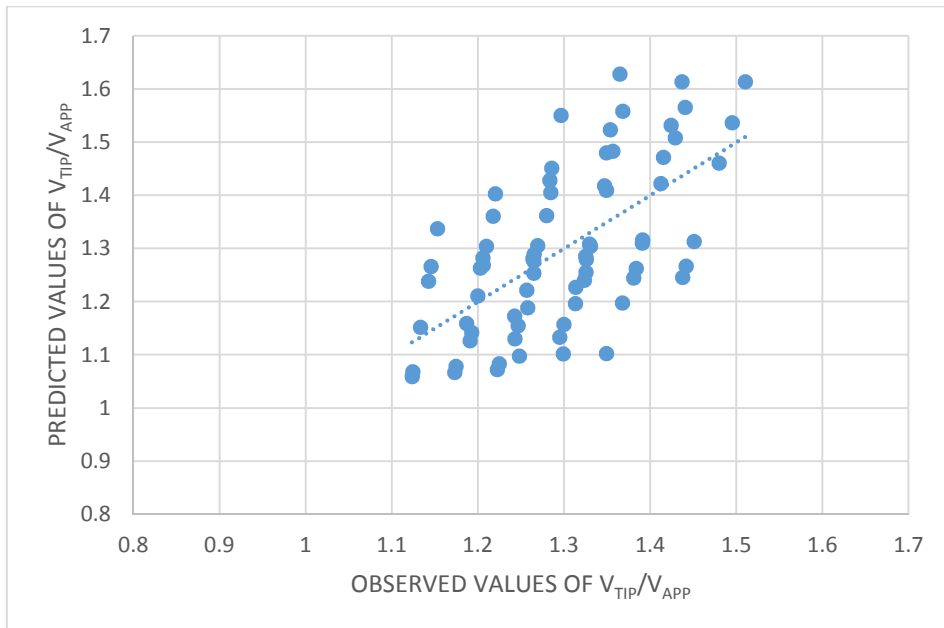
### 5.3.2 REGRESSION FOR TIP VELOCITY

i) In this analysis the dependent variable is  $V_{tip}/V_{app}$  and independent variable are Froude no.(Fr) , L/B.

SUMMARY OUTPUT						
<i>Regression Statistics</i>						
Multiple F	0.629015					
R Square	0.395659					
Adjusted R Square	0.378142					
Standard Error	0.120699					
Observations	72					
<i>ANOVA</i>						
	<i>df</i>	<i>SS</i>	<i>MS</i>	<i>F</i>	<i>Significance F</i>	
Regression	2	0.658111	0.329055	22.587	2.85E-08	
Residual	69	1.005216	0.014568			
Total	71	1.663327				
	<i>Coefficients</i>	<i>Standard Error</i>	<i>t Stat</i>	<i>P-value</i>	<i>Lower 95%</i>	<i>Upper 95%</i>
Intercept	0.709219	0.09059	7.828864	4.11E-11	0.528496	0.889941
Fr.	0.672174	0.17958	3.743037	0.000373	0.313922	1.030426
L/B	2.413133	0.521592	4.626474	1.69E-05	1.372585	3.453681

For the above analysis the correlation coefficient R comes out to be 0.629 which shows that the relation between variables is poor and thus there are some other factor playing a role in this. Further analysis is needed to get the factors influencing the maximum shear stress.





The scatter plot also shows clearly that the developed regression equation does not hold well with the results of this study. Thus further analysis is needed to get the factors influencing the tip velocity.

ii) In this analysis the dependent variable is  $V_{tip}/V_{app}$  and independent variable are Froude no.(Fr) , L/B and  $\theta_{net}$ .

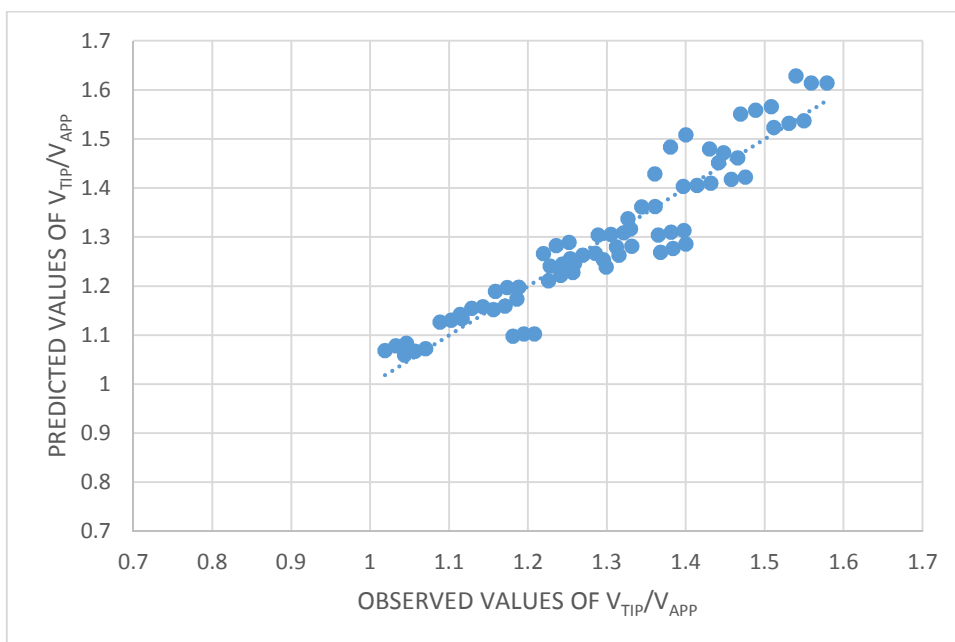
SUMMARY OUTPUT						
<b>Regression Statistics</b>						
Multiple R	0.946813					
R Square	0.896455					
Adjusted R Square	0.891887					
Standard Error	0.050327					
Observations	72					
<b>ANOVA</b>						
	<i>df</i>	<i>SS</i>	<i>MS</i>	<i>F</i>	<i>Significance F</i>	
Regression	3	1.491098	0.497033	196.2398	2.06E-33	
Residual	68	0.172229	0.002533			
Total	71	1.663327				
	<i>Coefficients</i>	<i>Standard Error</i>	<i>t Stat</i>	<i>P-value</i>	<i>Lower 95%</i>	<i>Upper 95%</i>
Intercept	1.052682	0.042255	24.91285	6.6E-36	0.968364	1.136999
Fr.	0.181427	0.079617	2.278737	0.025828	0.022553	0.340301
L/B	2.7255	0.218164	12.49291	2.83E-19	2.290161	3.160839
$\theta$	-0.77408	0.042684	-18.1351	9.43E-28	-0.85926	-0.68891

For the above analysis the correlation coefficient R comes out to be 0.9468 which shows that the relation between variables good and thus a regression equation can be developed. The value of adjusted R square comes out to be 0.9 which means 90% of the values fit the equation. The value of significance F is less than 0.05 which means the equation is

ok. Also all the P-values are less than 0.05 which means the independent variables used are good to be used.

Regression equation-

$$V_{tip}/V_{app} = 1.052682 + 0.181427Fr + 2.7255 L/B - 0.77408\theta$$



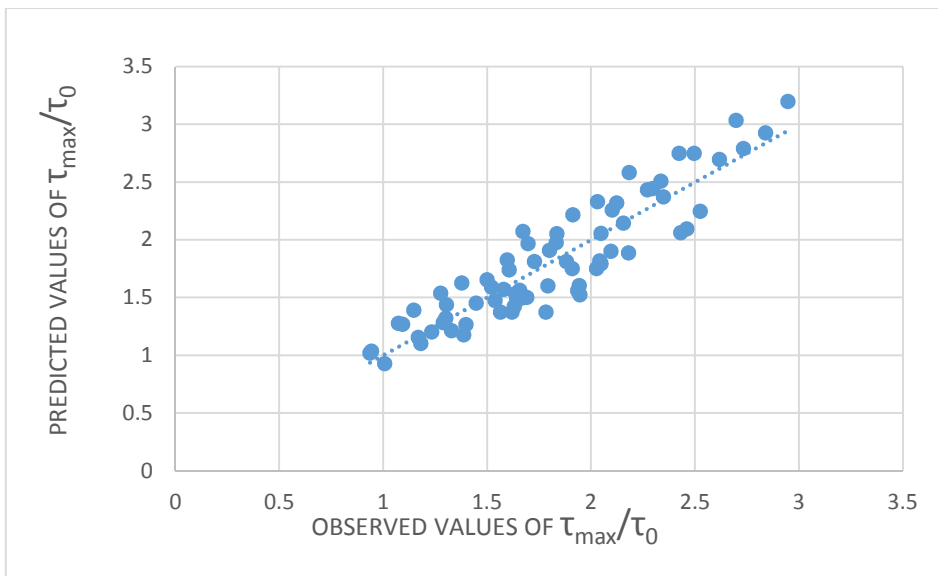
The scatter plot developed using above equation gives good linear relationship among the factors thus it can be used to predict the tip velocity at location of groyne.

### 5.3.3 REGRESSION FOR MAXIMUM SHEAR STRESS

i) In this analysis the dependent variable is  $\tau_{\max}/\tau_0$  and independent variable are Froude no.(Fr) and L/B.

SUMMARY OUTPUT						
<i>Regression Statistics</i>						
Multiple R	0.912373					
R Square	0.832424					
Adjusted R Square	0.827567					
Standard Error	0.218244					
Observations	72					
<i>ANOVA</i>						
	<i>df</i>	<i>SS</i>	<i>MS</i>	<i>F</i>	<i>Significance F</i>	
Regression	2	16.32549	8.162745	171.3767	1.72E-27	
Residual	69	3.286499	0.04763			
Total	71	19.61199				
<i>Coefficients</i>						
	<i>Standard Error</i>	<i>t Stat</i>	<i>P-value</i>	<i>Lower 95%</i>	<i>Upper 95%</i>	
Intercept	-0.77408	0.163802	-4.72572	1.17E-05	-1.10086	-0.44731
Fr.	4.7837	0.324709	14.73226	5.4E-23	4.135923	5.431477
L/B	7.272573	0.943123	7.711164	6.74E-11	5.391095	9.154051

For the above analysis the correlation coefficient R comes out to be 0.809 which shows that the relation between variables is not that good and thus there is some other factor playing a role in this. Further analysis is needed to get the factors influencing the maximum shear stress.



It can also be seen that the scatter plot between predicted and observed values is fair but not good.

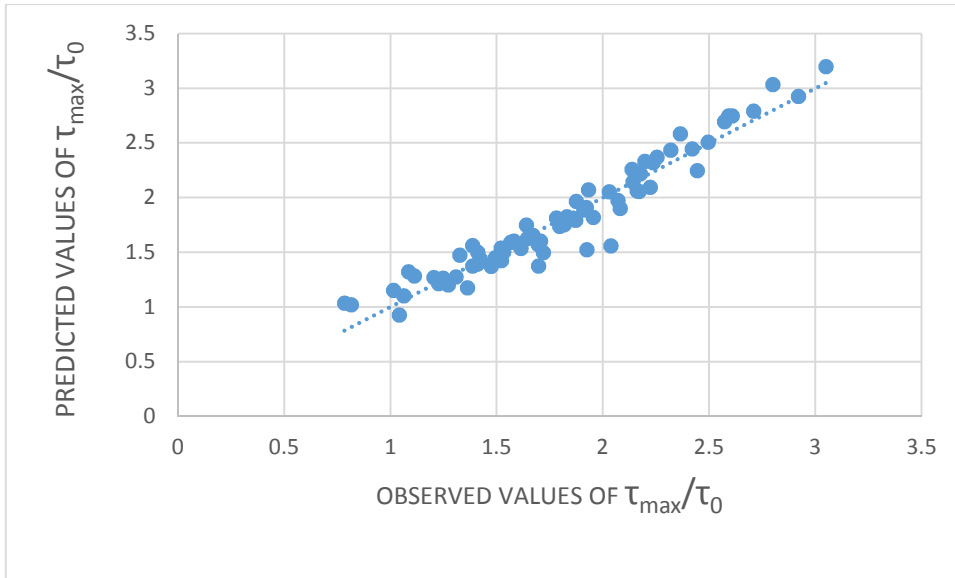
ii) In this analysis the dependent variable is  $\tau_{\max}/\tau_0$  and independent variables are Froude no. (Fr), L/B and  $\theta_{\text{net}}$

SUMMARY OUTPUT						
<i>Regression Statistics</i>						
Multiple R	0.963959					
R Square	0.929217					
Adjusted R Square	0.926094					
Standard Error	0.14288					
Observations	72					
<i>ANOVA</i>						
	<i>df</i>	<i>SS</i>	<i>MS</i>	<i>F</i>	<i>Significance F</i>	
Regression	3	18.2238	6.074599	297.5616	5.07E-39	
Residual	68	1.388192	0.020415			
Total	71	19.61199				
	<i>Coefficients</i>	<i>Standard Error</i>	<i>t Stat</i>	<i>P-value</i>	<i>Lower 95%</i>	<i>Upper 95%</i>
Intercept	-0.25559	0.119962	-2.13056	0.036745	-0.49497	-0.01621
Fr.	4.042865	0.226037	17.88588	2.06E-27	3.591815	4.493914
L/B	7.744124	0.619376	12.50311	2.72E-19	6.508179	8.980069
$\theta$	-1.16856	0.121182	-9.64301	2.36E-14	-1.41038	-0.92675

For the above analysis the correlation coefficient R comes out to be 0.964 which shows that the relation between is acceptable. The value of adjusted R square comes out to be 0.93 which means 93% of the values fit the equation. The value of significance F is less than 0.05 which means the equation is ok. Also all the P-values are less than 0.05 which means the independent variables used are good to be used. Thus a regression equation can be developed.

Regression equation-

$$\tau_{\max}/\tau_0 = -0.25559 + 4.042865Fr + 7.744124L/B - 1.16856\theta$$



The above scatter plot gives a good relation between observed and predicted values of maximum shear stress thus an empirical regression equation can be used. This equation can thus be used to find the bed shear stress at any location of groyne.

From the above analysis it can be said that the maximum shear stress depend on Froude Number, location of groyne, groyne length. Keeping in view the above information the best placement combination of groynes in the simulated bend is predicted below.

#### 5.4 VARIATION OF FACTOR $V_{tip}/V_{app}$ WITH FACTOR $L/B$ FOR DIFFERENT POSITION OF THE GROYNES.

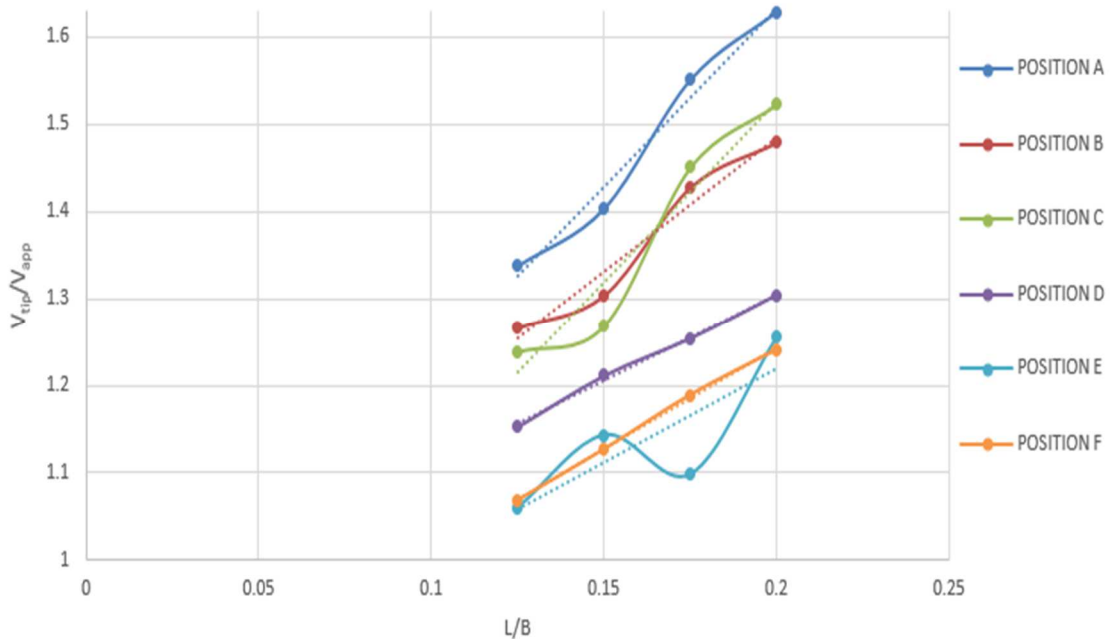


FIG. 5.1 Variation of  $V_{tip}/V_{app}$  with  $L/B$  for velocity 1.4m/s.

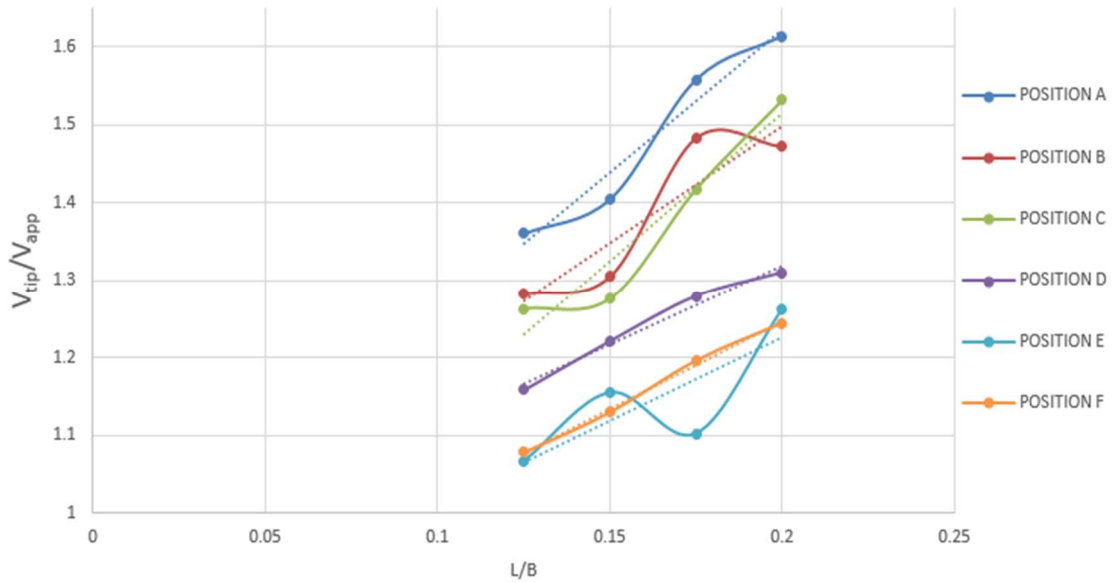


FIG.5.2 Variation of  $V_{tip}/V_{app}$  with  $L/B$  for velocity 2 m/s.

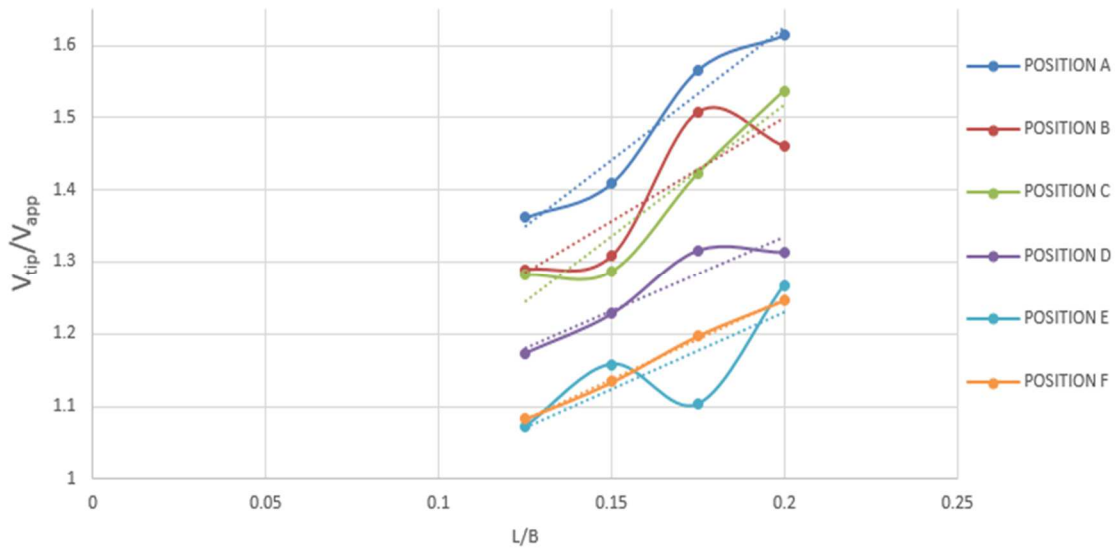


FIG.5.3 Variation of  $V_{tip}/V_{app}$  with  $L/B$  for velocity 2.6 m/s.

It can be observed that the variation is not linear, as expected there are other factors that influence the Tip Velocity. It can be inferred from the variation that with increase in  $L/B$  ratio the Value of  $V_{tip}/V_{app}$  increases for almost all the cases of placement of groynes.

The position that should be noted is position 5, for an  $L/B$  ratio of 0.175, that is Length of groyne=3.5m. At this position for all the velocities of flow it can be seen that there is sudden drop in the  $V_{tip}/V_{app}$  factor or the tip velocity. The tip velocity the maximum velocity that is found near the groyne and thus it contributes to the formation of vortices that lead to scouring.

Owing to the curvature of the section it can be seen that the velocities here also contribute to the production of centrifugal forces on the bend which in turn will cause more scouring. Free vortex is formed where the curvature is more and where the tip velocity is maximum thus creating more disturbances as that might be observed in a straight channel.

It should also be noted that the position of this tip velocity is very near to the position of maximum bed shear stress. Thus variation of shear stress with length of groyne was also needed to be studied, as the above analysis cannot on its own determine a good placement.

### 5.5 VARIATION OF FACTOR $\tau_{max}$ FOR DIFFERENT GROUYNE POSITION.

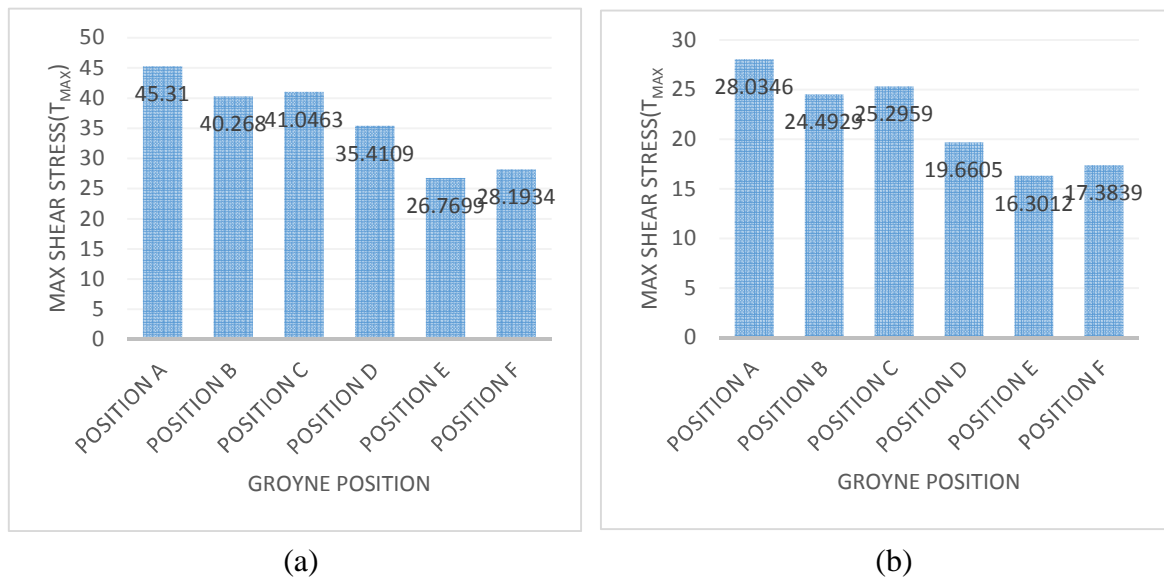
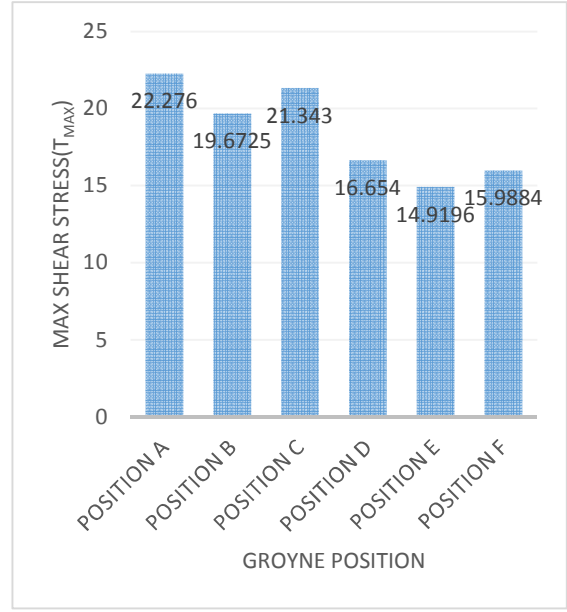
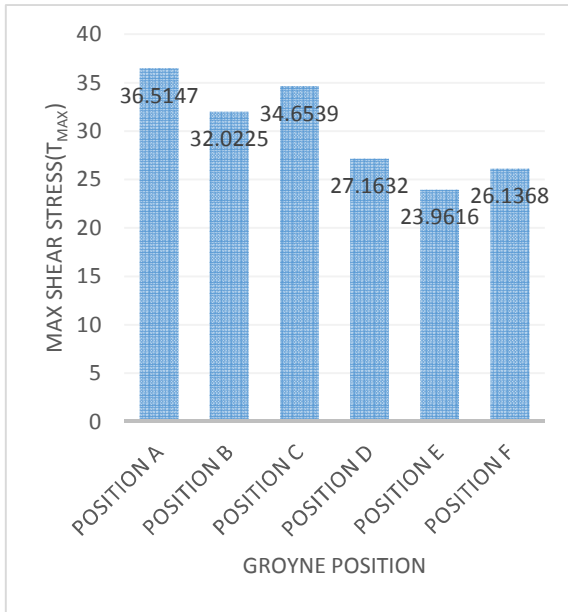
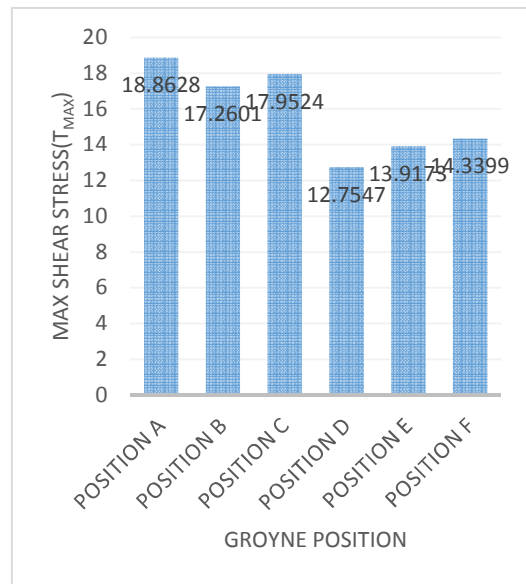
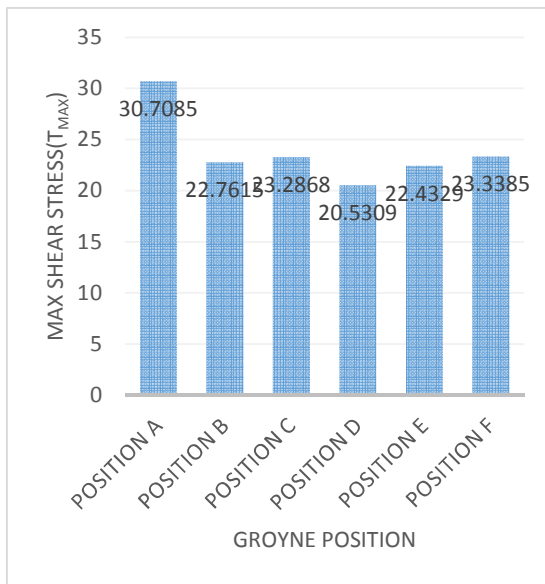


FIG 5.7  $\tau_{max}$  for groyne size 3.5m a) velocity 2.6m/s b) velocity 2m/s



(a)

(b)

FIG 5.7  $\tau_{max}$  for groyne size 3m a) velocity 2.6m/s b) velocity 2m/s

(a)

(b)

FIG 5.7  $\tau_{max}$  for groyne size 2.5m a) velocity 2.6m/s b) velocity 2m/s

Analysis of the above variation shows that the maximum shear stress reduces with decrease in groyne size. Thus a maximum value of 47.8 Pa was observed for groyne size of 4m and minimum shear stress of for groyne size 22.43 Pa for velocity of 2.6m/s. It can also be seen that in each case for various groyne size and velocities the minimum value occurs at position 'E'. This shows that this position is the most efficient among all the position.



## 5.6 SUMMARY

The above analysis of factors that influence the flow in a channel bend gives an idea of which position or placement of groyne is the most suited. Position “E” that is attracting at  $20^{\circ}$  and repelling at  $45^{\circ}$ , with respect to decided meridian “OP” gives the minimum bed shear stress, low tip velocity and considerably good protected length.

For this position the tip velocity varies from 1.26 times to 1.07 times as size varies from 4m to 2.5m. Whereas the maximum shear stress varies from 2.09 times the undisturbed shear stress (14.94 Pa) to 1.5 times for different sizes. Thus on the basis of this study it is the best placement of groyne combination to pass the flow through the channel bend safely.

Suggestion for the groyne size can be also given based on the trend seen in the various factors during the iterations. Groyne size of 3.5m gives considerable good results when employed at position ‘E’ in this channel bend.

## CHAPTER 6

### CONCLUSION

#### 6.1 INTRODUCTION

This chapter indexes the conclusions that are made based on analysis of the results obtained and the relationship derived among the various factors involved. The factors that are understood to be most important for the complex flow in a channel bend are mentioned below.

After sincere analysis of the inferences and the data obtained, the best placement of groynes is also predicted, that protects the bend in the most efficient way.

#### 6.2 CONCLUSIONS BASED ON PROTECTED LENGTH.

The protected length (D), which is the length of the concave bend of the section that was protected after the introduction of the groyne is an important factor for the flow. The variation of this factor can in itself throw some light on the placement of groyne that is giving the best results.

It is seen that the protected length depends on the position of the groyne. Through the relationship or variation is not linear, the maximum value of 'D' is observed for position 'E' and position 'F'.

POSITION 'E'	POSITION 'F'
attracting groyne at 45 <sup>0</sup> and repelling groyne at 20 <sup>0</sup> with respect to meridian "OP"	attracting groyne at 60 <sup>0</sup> and repelling groyne at 35 <sup>0</sup> with respect to meridian "OP"

TABEL 6.1 FOR REFERENCE

Where, **D (position 'F') > D (position 'E')** for all velocities, 2.6m/s; 2m/s; 1.4m/s.

This analysis helps us narrow down our field of vision to choose the best placement, to position E or position F.

#### 6.3 CONCLUSIONS BASED ON TIP VELOCITY.

The tip velocity is the velocity near the tip of the groyne on the concave bank. This velocity has significance to understand local scouring, its extent and location.

It is seen that the variation of factor with  $V_{tip}/V_{app}$  is increasing with increase in groyne size. It can be inferred from the variation between  $V_{tip}/V_{app}$  and L/B that the minimum values of tip velocity ratio is for position 'E' and position 'F'. Thus in concurrence with the above inference, position 'E' and 'F' are the more efficient position among others. It can also be seen from the variation of  $V_{tip}/V_{app}$  vs. L/B that there is a sudden drop in the value of tip velocity ratio at position 'E' and this is very close to the absolute minimum value of  $V_{tip}/V_{app}$  for any position.

Thus we can say that out of position 'E' and position 'F', the former is more efficient.

Also, it can be noted that this minimum value occurs at L/B ratio of 0.175 that is for, groyne size of 3.5m.

#### **6.4 CONCLUSIONS BASED ON MAXIMUM BED SHEAR STRESS.**

Maximum bed shear stress is a critical factor for the flow in a channel bend. This helps in scouring and its extent that will take place. The bed shear stress in this study was found to be maximum always near the groyne, thus suggesting the location of local scour.

As expected the value of maximum shear stress reduced as the approach velocity varied from 2.6m/s;2m/s to 1.4m/s. Though the relation with the different positions of the groyne was not linear and local minimum, local maximum was found in the data. For location 'E' the minimum value of bed shear stress was found among all the position of groyne placement for different groyne sizes. This suggests that the placement 'E' is the most effective among the other positions.

#### **6.5 SUGGESTION FOR THE BEST PLACEMENT OF GROYNES.**

After analysis of the factors involved and their relationship among themselves, an efficient placement of groyne can be established with an appreciable confidence.

The position "E" that is attracting at  $20^0$  and repelling at  $45^0$ , with respect to decided meridian "OP". is the most efficient placement among all the postions. This positions gives the minimum value of bed shear stress and tip velocity simultaneously providing a high value of protected length over concave bank.

Also certain suggestion can be given for the appropriate length of the groyne. The factors maximum shear stress, tip velocity and protected length are found to in appreciable range for L/B ratio of 0.175 that is groyne size of 3.5m.

#### **6.6 FURTHER IMPROVEMENTS**

- a) For the positions of the groyne placement decided, it would be appreciable if more iterations can be done on the orientation groyne with respect to direction of flow, as it was assumed constant for this study.
- b) The width of the channel and Radius of curvature of bend can also be varied to get more variations and derive factors to get better results.
- c) Different models for analysis can be applied that are available in Ansys Fluent like Large Eddy Simulation, which may give better results.

## REFERENCES/BIBLIOGRAPHY

1. Suharjoko, *Study on Numerical Modeling of Two-Dimensional Horizontal Flow special case Groyne on the River Estuary*, Thesis for the degree of Master Science in Civil Engineering Program, Department of Engineering Science, Post-graduate Program, University Of Gajah Mada, Yogyakarta, 1999.
2. Suharjoko, 2001, *Numerical Modeling of Two-Dimensional Horizontal Flow on Groyne Field due to Groyne Placement on the River Straight*, Researches Report, Departemen of Research and Applications, Institute of Technologie Sepuluh Nopember, Surabaya, 2001.
3. Kashyap, Shalini. *NUMERICAL MODELING OF FLOW AROUND SUBMERGED GROYNES IN A SHARP BEND USING LARGE EDDY SIMULATION*. Diss. University of Ottawa, 2010.
4. Jungseok Ho, Hong Koo Yeo, Julie Coonrod, and Won-Sik Ahn, *NUMERICAL MODELING STUDY FOR FLOW PATTERN CHANGES INDUCED BY SINGLE GROUYNE*, Seminario Internacional La Hidroinformática en la Gestión Integrada de los Recursos Hídricos, Universidad del Valle/Instituto Cinara Kutija, V. and Murray, M. G. 162 , 2005.
5. Heereveld ,Zijlstra, *RIVER GROYNES FOR THE FUTURE innovative groyne design*, EU Water Framework Directive, EU Habitats Directive. 2006.
6. Prohaska Sandra (2007), Thomas Jancke, Bernhard Westrich, *MODEL BASED ESTIMATION OF SEDIMENT EROSION IN GROUYNE FIELDS ALONG THE RIVER ELBE*, University of Stuttgart, Institute of Hydraulic Engineering, Stuttgart, Germany, 2006.
7. Duan, J.G., Nanda, P., 2006, *Two-dimensional depth-averaged model simulation of suspended sediment concentration distribution in a groyne field*, Journal of Hydrology, Elsevier, (2006).

8. Zhang Hao, Hajime Nakagawa, Yasunori Muto, Yosio Muramoto, et al, *Morphodynamics of Channel with Groins its Applications in River Restoration*, Annual of Disas, Prev. Res. Inst. Kyoto Univ., No. 50 B. 2007.
9. Armani A, M. Righety, Sartori F, *Experimental Analysis of Fluvial Groyne*, Proc, of River Flow, Braunschweig, (2010).
10. Zhang Hao, Mizutani and Nakagawa, *Impact of Grain Size Distribution on Bed Topography around a Groyne*, 34th IAHR world Congress – Balance and Uncertainty, ISBN 978-0-85825-868-6, Brisbane, Australia, 26 June-1 July 2011.
11. Thacker, Ben H., Scott W. Doebbling, Francois M. Hemez, Mark C. Anderson, Jason E. Pepin, Edward A. Rodriguez. LA-14167-MS, Issued, “*Concepts of Model Verification and Validation*”, Edited by Charmian Schaller, Approved for public release;IM-1. Los Alamos National Laboratory, is operated by the University of California for the United States Department of Energy under contract W-7405-ENG-36, (October 2004).
12. Triatmadja R, *Numerical and physical studies of Shallow Water Wave with special reference to Lanslate generated Wave and the method of Characteristics*, Department of Civil Engineering University of Strathclyde, Glasgow, United Kingdom(1990).
13. Nur Yuwono, *Hydraulics Modeling*, Central of University Association on Engineering Science, University Of Gajah Mada, Yogyakarta., 1994.